Petrology, Vol. 7, No. 3, 1999, pp. 267–288. Translated from Petrologiya, Vol. 7, No. 3, 1999, pp. 276–298.

Petrology and Tectono-Thermal Evolution of Granulites in the Bryansk Block, Voronezh Crystalline Massif

K. A. Savko

Voronezh State University, Universitetskaya pl. 1, Voronezh, 394693 Russia
e-mail: gfkig304@main.vsu.ru

Received July 27, 1998

Abstract—The Early Archean granulites of intermediate composition in the Bryansk block, Voronezh crystalline massif, contain reaction textures of small garnet grains, which were formed by the reaction *Opx* + *Pl* ⟶ *Grt* + *Qtz* during isobaric cooling. The *P–T* conditions of the metamorphic culmination for granulites in the eastern portion of the block were estimated at 788–823°C and 5.3–5.5 kbar, and the corresponding values for granulites in the western part of the block were 850°C and 5.5–6 kbar, which corresponds to a depth of 20–22 km. The retrograde alterations ceased at a temperature of about 600°C and pressures of 2.9–3.0 kbar (at depths of ~10 km). The *P–T* paths constructed on the basis of thermometric data on granulites from the western and eastern portions of the area are similar, a fact indicating that the Bryansk block evolved as a single structure. Although reaction textures in the granulites provide evidence of the isobaric cooling of the rocks, their *P–T* paths correspond to a geothermal gradient of 1.2 kbar/100°C (20°C/km) and pass between typical isothermal decompression (ITD) and isobaric cooling (IBC) trends. Petrological and seismic data suggest the following model for successive geologic events within the Bryansk block during Archean time: (1) subsidence of the block and sedimentation; (2) collision and associated magmatism and tectonic thickening of the crust, prograde metamorphism, and subisobaric cooling; and (3) erosion-related exhumation of the granulite complex and the cessation of active rock recrystallization (due to the deterioration of fluid activity) at a depth of about 10 km.

INTRODUCTION

An important problem of metamorphic petrology is the thermal regime of the subsidence and uplift stages of granulite complexes. This information can be derived from mineral assemblages that are now open to examination. In this connection, it is particularly interesting to examine the evolution of ancient Precambrian shields, whose thermal regimes were basically different from the regimes of zonal metamorphic complexes in Phanerozoic foldbelts.

In contrast to many thoroughly studied Precambrian granulites of the Russian Platform, the Archean granulites of the Voronezh crystalline massif remained a blind-spot up to quite a recent time. Researchers of the massif have long debated the problem of whether the massif includes rocks metamorphosed to the granulite facies, and, although many geologists actually used the term *granulite* in their papers, there was no clear petrological evidence of the presence of these rocks. The types of rocks that could be regarded as granulites were uncertain, their mineral assemblages were not examined, and there were no consistent estimates of the *P–T* metamorphic conditions. At the same time, many researchers denied the presence of granulites among the rocks of the Voronezh crystalline massif, referring to the uncertainty of the boundary between the amphibolite and granulite facies. The presence of granulites in the massif was proved by the discovery of gneisses and metapelites with the *Grt* + *Crd* + *Kfs* and *Crd* + *Hyp* + *Or* assemblages.

The Voronezh crystalline massif is known to consist of two Archean blocks, which are made up of rocks metamorphosed to the granulite facies: the Kursk–Besedino and Bryansk blocks. The granulites of these blocks are diverse in composition. The Kursk–Besedino block is dominated by eulysites, metabasics, metaultrabasics, and metapelites. The Bryansk block contains widespread granulites of intermediate composition ("metadiorites"), metapelite, eulysites, and marbles.

This paper is centered on the mineral assemblages and reaction textures in the Early Archean granulites from the eastern and western portions of the Bryansk block. The data obtained on the rocks were employed to determine their *P–T* paths and reconstruct the thermo-tectonic crustal evolution in the Early Archean.

GEOLOGY

The Bryansk Archean block (Fig. 1) composes the northwestern part of the Voronezh crystalline massif, which is a buried uplift of the Precambrian basement of the Russian Platform. The block accounts for approximately 1/5 of the massif by area, i.e., for about 100000 km^2. The crystalline basement is overlain by a cover of Phanerozoic sediments, whose thickness attains 320–640 m. Because of this, the very first data

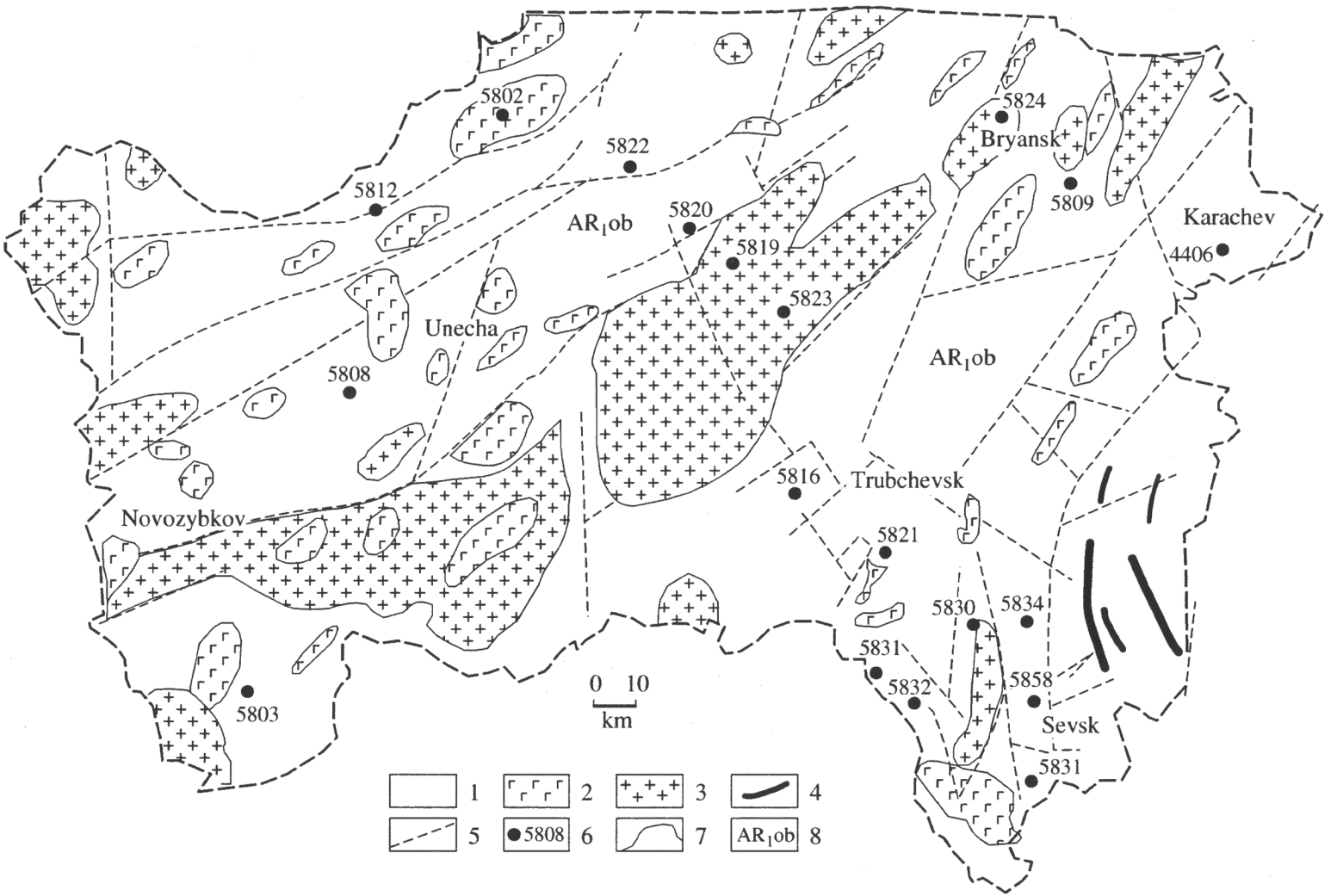

Fig. 1. Schematic geological map of the Bryansk block, Voronezh crystalline massif.

(1) Gneisses of intermediate composition, calc–silicate rocks, marbles, aluminous graphite gneisses, and quartzites; (2) gabbroids; (3) granitic rocks; (4) eulysites; (5) faults; (6) drill holes and their numbers; (7) geologic boundaries; and (8) Oboyan' Group.

on the geology of the Bryansk block were obtained as recently as the 1970s in the course of deep geological surveying and mapping to a scale of 1 : 500000, when granulites were penetrated by some drill holes. Until now, there are only thirteen holes that penetrated the crystalline basement for relatively large depths (up to 400 m).

Seismic data indicate that, in contrast to other structures of the Voronezh crystalline massif, the Bryansk block has no boundary with velocities of 6.3–6.7 km/s (this boundary is the first beneath the crystalline basement surface in other structures; Golionko and Krestin, 1973). This is explained by the fact that the surface of the Bryansk block is made up of deeply eroded rocks of intermediate and mafic composition, whose densities and seismic velocities approach those of the basaltic layer. The boundary was detected in all other structures of the Voronezh Massif, in which it occurs at depths of 3–7 km. The Early Archean structures of the Bryansk block are gently dipping depressions and dome-shaped uplifts with dip angles of 5°–20°.

The rocks composing the Precambrian basement of the block are provisionally attributed to the most ancient rocks of the Voronezh crystalline massif, the Oboyan' Group (which is also referred to as the Bryansk Group) of the Early Archean (Shchegolev, 1985; Nozhkin and Krestin, 1984; etc.). Unfortunately, the Bryansk granulites have not been precisely dated isotopically as of yet.

PETROGRAPHY

In the western part of the Bryansk block, granulites were recovered by Hole 5808. The rocks comprise two main types: plagioclase–quartz–sillimanite–biotite–garnet and plagioclase–quartz–biotite–orthopyroxene–garnet massive or slightly banded, medium- to coarse-granular gneisses of light gray to gray color. The textures of the rocks are granoblastic, lepidogranoblastic, or porphyroblastic, with porphyroblasts of large garnet grains, which sometimes account for up to 40%. The mineral assemblages of the granulites are listed in Table 1. In the east of the block, Hole 5809 penetrated orthopyroxene–garnet granulites of intermediate composition, which are dominated by plagioclase and contain orthopyroxene, garnet, potassium feldspar, and biotite. Quartz occurs in the rocks only near contacts between orthopyroxene and garnet.

A representative stratigraphic column of the Precambrian can be studied in materials recovered by only thirteen drill holes, which will be briefly characterized below. Hole 5833 (Fig. 1) penetrated intercalating acid (*Grt* + *Pl* + *Qtz* + *Bt*) and feldspar (*Pl* + *Grt* + *Opx* + *Kfs* + *Bt*) gneisses and calc–silicate rocks. Hole 5835 passed through intercalating metapelitic gneisses (*Qtz* + *Pl* + *Sil* + *Bt* + *Crd* + *Kfs* + *Ilm*), calc–silicate (*Cpx* + *Hbl* + *Pl* + *Kfs* ± *Cal*) rocks, eulysites (*Qtz* + *Opx* + *Mag* ± *Cpx* ± *Cum*), and thin layers of metabasites (*Cpx* + *Hbl* + *Pl* + *Spn*). Hole 5830 recovered metapelites (*Qtz* + *Pl* + *Kfs* + *Crd* + *Bt* ± *Sil* ± *Grt*), migmatites, and plagioclase amphibolites. Hole 5821 penetrated through a sequence of peraluminous quartzites (*Qtz* + *Bt* ± *Crd* ± *Sil* ± *Kfs*), metapelites (*Qtz* + *Pl* + *Kfs* + *Crd* + *Bt* + *Sil*), and migmatites. Finally, Hole 5816 recovered peraluminous graphite-bearing gneisses (*Qtz* + *Crd* + *Sil* + *Gr* + *Bt* + *Kfs*).

The Bryansk block contains widely spread calc–silicate rocks and phlogopite–diopside marbles, which were described in detail in our earlier paper devoted to the petrology of the magnesian marbles (Savko and Lebedev, 1996).

Petrologically significant textures of the intermediate granulites from the eastern part of the Bryansk block are the following growth textures of the garnet:

(a) inclusions of small euhedral garnet grains (*Grt*-II) in large orthopyroxene crystals with quartz inclusions (Figs. 2a, b);

(b) newly formed garnet (*Grt*-III), often in association with quartz grains, at contacts between orthopyroxene, orthoclase, and plagioclase (Fig. 2b); and

(c) inclusions of tiny euhedral garnet grains (*Grt*-IV) along the contacts of large plagioclase crystals with orthopyroxene grains in Sample 5809/3 (Fig. 2a).

The newly formed garnet contains no inclusions other than biotite. In places, the rock bears plagioclase–quartz myrmekite (Sample 5908/3, Fig. 2a). The reaction textures listed above provide evidence of the reaction

$$Opx + Pl \longrightarrow Grt + Qtz. \quad (1)$$

Which results in garnet growth with increasing pressure or cooling of the rocks. The garnet growth textures are interpreted as secondary, overprinted on high-temperature assemblages, when the *P–T* conditions changed after the metamorphic climax.

The retrograde textures in gneisses from the western portion of the Bryansk block are pronounced not as clearly as in rocks in the eastern part, but the growth of later garnet (*Grt*-II) at contacts with large crystals of primary garnet (*Grt*-I) suggests the reaction

$$3An \longrightarrow Grs + 2Sil + Qtz, \quad (2)$$

which reflects subisobaric cooling and is associated with a decrease in the Ca mole fraction of the plagioclase at its contacts with garnet. In the orthopyroxene-bearing gneiss (Sample 5808/7), the decrease in the Ca mole fraction of the plagioclase (by 6–10 mol % *An*) also suggests reaction (1).

ANALYTICAL TECHNIQUES

All granulite samples were selected from the core of drill holes, which was thoroughly described during fieldwork. The samples were first examined with an optic microscope. Microprobe analyses of minerals were made on a Camebax SX-50 microprobe at the

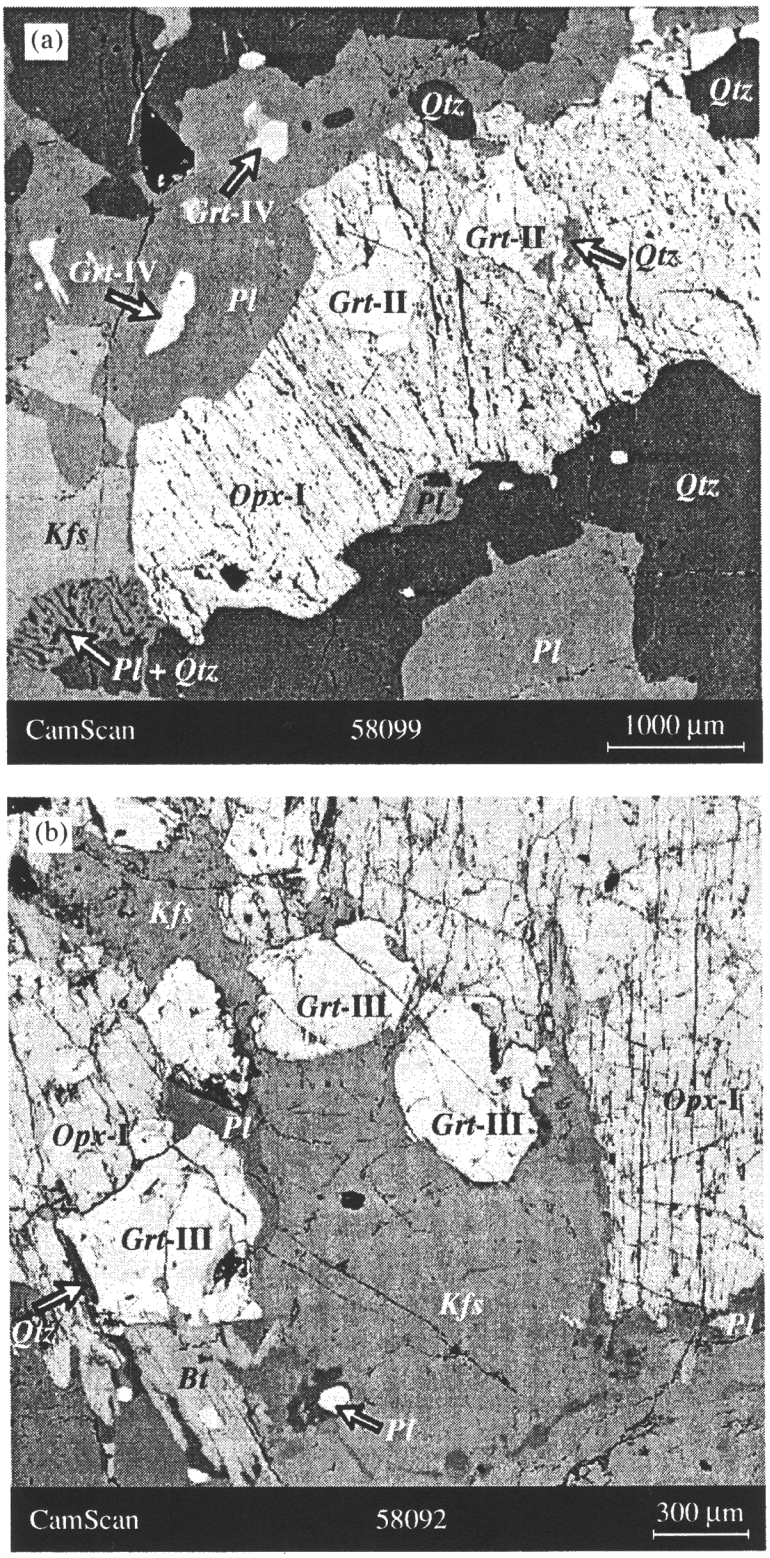

Fig. 2. Back-scattered electron images showing different garnet types from granulites in the eastern part of the Bryansk block.
(a) Inclusions of newly formed garnet (*Grt*-II) in orthopyroxene (*Opx*-I); small garnet grains (*Grt*-IV) are included in plagioclase; Sample 5809/3.
(b) Newly formed small garnet grains (*Grt*-III) at contact with orthopyroxene (*Opx*-I); Sample 5809/1.
Images were taken on a CamScan electron microscope.

Moscow State University at an accelerating voltage of 15 kV, with a beam current of 1–2 nA, and a beam 1–2 μm in diameter. The accuracy of the analyses was systematically controlled using synthetic and natural standards. Back-scattered electron images of the reaction textures were taken on a CamScan electron micro-

scope at the Moscow State University. The numbers of cations were normalized to 12 oxygens for garnet, 6 for orthopyroxene, 8 for garnet, and 11 for biotite.

MINERALOGY

The mineral assemblages of high-temperature rocks of the Bryansk block are listed in Table 1, and representative analyses of minerals are given in Tables 2–5.

Granulites of the Eastern Part of the Bryansk Block

Orthopyroxene. According to the grain size, composition, and zoning patterns, the mineral can be subdivided into two groups.

(1) Large (4–5 mm) grains of aluminous pyroxene (*Opx*-I, Samples 5809/1, 5809/3, 5809/11; Figs. 2a, 2b, and 3a), which show a clear tendency of Al_2O_3 contents decreasing from 3.23–4.02 wt % in the cores to 2.49–3.16 wt % in the margins, regardless of adjacent minerals, with the difference in the Al_2O_3 contents remaining nearly unchanged (Table 2). No zoning in the distribution of Fe and Mg was detected, with the Mg mole fraction (X_{Mg}) of the mineral ranging from 0.522 to 0.569 and occasionally slightly increasing at contacts with garnet inclusions (from 0.522 to 0.546 in Sample 5809/1).

(2) Small orthopyroxene crystals (*Opx*-II) with lower Al_2O_3 contents (2.18–2.75 wt %) and without zoning. A dependence was detected between the size of orthopyroxene grains and the Al mole fraction of the mineral, with smaller grains showing lower Al_2O_3 contents. The aluminum mole fraction of small orthopyroxene grains is generally close to this parameter in the margins of large crystals. Smaller grains are more magnesian, with this parameter increasing with decreasing grain size (Sample 5809/4). Zoning was detected in the orthopyroxene only at its contacts with garnet, where X_{Mg} notably increases (from 0.577 to 0.606 in Sample 5809/4, Table 2).

Garnet. Four groups of the mineral were recognized based on its morphology, genesis, and zoning.

(1) Large grains (*Grt*-I), sometimes with inclusions of biotite and quartz, relatively magnesian (X_{Mg} = 0.306–0.327), homogeneous, except thin outermost zones, in which the Mg mole fraction depends on minerals occurring at contacts with the garnet grain (Table 3). The Mg mole fraction of a large garnet grain (Sample 5809/11, Fig. 3a) decreases to 0.267–0.269 at its contacts with hypersthene and biotite and almost does not change (0.304) at contacts with plagioclase. In terms of Ca contents, the garnet is homogeneous. The garnet of Sample 5809/4 has X_{Mg} equal 0.310 in the core (Table 3), 0.276 at contacts with biotite, and 0.306–0.308 at contacts with small orthopyroxene grains and plagioclase. No zoned Ca distribution was detected in the garnet of Sample 5809/11, whereas this mineral in Sample 5809/4 shows somewhat higher grossular contents in the margin, regardless of adjacent minerals. No zoning in the distribution of Mn was observed.

Table 1. Mineral assemblages of the studied rocks from the Bryansk block of the Voronezh crystalline massif

Sample number	Mineral assemblage
5808/4	*Pl + Grt + Bt + Qtz + Sil*
5808/7	*Pl + Grt + Qtz + Opx + Bt + Kfs*
5809/1	*Pl + Opx + Grt + Kfs + Bt + Qtz + Ilm*
5809/3	*Pl + Opx + Grt + Kfs + Qtz*
5809/4	*Pl + Opx + Grt + Kfs + Bt + Qtz + Ilm*
5809/11	*Pl + Opx + Grt + Kfs + Bt + Qtz*

(2) Small euhedral homogeneous garnet grains (*Grt*-II) included in orthopyroxene. Their composition is more ferrous than that of larger *Grt*-I: the cores have X_{Mg} = 0.273–0.285 (Samples 5809/1, 5809/3, Fig. 2a, Table 3). Most of these garnet grains are zoned, with X_{Mg} decreasing (to 0.258–0.269) from the cores to margins of grains. Their zoning patterns are different from those of large crystals. This type of garnet (*Grt*-II) is characterized by a gradual decrease in X_{Mg} toward contacts with orthopyroxene. No regularities in the variations of Ca concentration were detected. For example, the grossular content increases from 0.046 in the core to 0.059 in the margin in one of two garnet inclusions in orthopyroxene (Sample 5809/3, Fig. 3a) and almost does not change in the other inclusion (0.050 and 0.053, respectively). The Mn mole fraction somewhat increases toward the margins.

(3) Small and medium-sized euhedral garnet grains (*Grt*-III) at contacts of orthopyroxene grains with other minerals (Fig. 2b). Their Mg mole fractions are similar to those of garnet inclusions in orthopyroxene, but they are devoid of zoning in the contents of Mg and Fe. A decrease in X_{Mg} (from 0.288 to 0.262) was detected only in one garnet grain of medium size at its contact with biotite (Fig. 2b), with the composition of the garnet remaining unchanged at contacts with other minerals. Garnet grains armored with ilmenite and plagioclase are almost unzoned in terms of Mg and Fe contents, but their concentrations of grossular slightly increase from the core ($Grs_{0.050}$) to margin ($Grs_{0.059}$).

(4) Very small euhedral garnet grains (*Grt*-IV) in plagioclase (Sample 5809/3, Fig. 2a), whose Mg mole fractions are 0.285–0.302 in the cores and decrease toward the margin to 0.239. The grossular concentrations increase toward the margins from 0.051 to 0.060).

Plagioclase. Plagioclase occurs in the rocks as crystals of various sizes in the groundmass of the rock, inclusions in orthopyroxene, and plagioclase–quartz

Table 2. Composition (wt %) of orthopyroxene from granulites of the Bryansk block, Voronezh crystalline massif

Component;	5809/11			5809/4						5809/1					5809/3		5808/7	
	large grain			large grain			small grain			large grain		small grain			large grain		small grain	
	core	core	margin, near *Grt*	core	core	margin, near *Grt*	margin, near *Pl*	margin, near *Grt*	core	core	margin, near *Pl*	core	margin, near *Qtz*	margin, near *Grt*	margin, near *Pl*	core	core	margin, near *Grt*
	1	2	3	4	5	6	7	8	9	10	11	12	13	14	15	16	17	18
SiO_2	50.25	49.96	50.68	51.26	50.48	51.23	51.64	52.00	52.19	49.73	50.74	50.78	50.30	50.22	51.06	50.53	49.79	49.78
TiO_2	–	–	–	0.13	0.09	0.09	0.12	0.10	0.10	0.12	0.08	0.08	0.13	0.09	–	–	0.07	0.05
Al_2O_3	3.23	3.94	2.76	3.60	3.57	2.93	2.11	2.36	2.18	3.72	2.49	2.71	2.75	2.59	3.16	4.02	1.11	0.95
Cr_2O_3	0.31	0.04	–	0.16	0.16	0.12	0.03	0.05	0.03	0.07	–	0.08	0.11	–	0.26	0.23	0.10	–
FeO	26.66	28.24	26.82	25.57	26.10	25.91	25.67	23.89	24.66	28.78	27.68	26.49	27.32	28.55	26.39	26.45	32.82	33.45
MnO	–	0.32	–	0.16	0.18	0.11	0.14	0.23	0.10	0.32	0.20	0.21	0.19	0.10	0.36	0.36	0.46	0.39
MgO	19.56	17.74	19.74	18.61	18.29	18.81	19.63	20.64	19.54	17.64	18.64	20.08	19.47	18.03	19.03	18.64	15.38	15.25
CaO	–	–	–	0.20	0.19	0.20	0.23	0.21	0.23	0.19	0.17	0.16	0.16	0.19	–	–	0.029	0.31
Na_2O	–	–	–	–	0.04	–	–	–	0.08	–	–	0.05	0.02	–	–	–	0.01	0.08
K_2O	–	0.02	–	0.02	0.01	0.01	0.02	0.01	0.01	–	0.03	0.02	0.01	–	–	–	–	–
Total	100.01	100.26	100.00	99.72	99.11	99.41	99.59	99.49	99.12	100.57	100.03	100.66	100.46	99.77	100.26	100.23	100.03	100.26
Si	1.908	1.906	1.923	1.937	1.928	1.946	1.957	1.955	1.975	1.899	1.935	1.916	1.910	1.929	1.930	1.911	1.955	1.955
Ti	–	–	–	0.004	0.003	0.003	0.003	0.003	0.003	0.003	0.002	0.002	0.004	0.003	–	–	0.001	0.001
Al(IV)	0.092	0.094	0.077	0.063	0.072	0.054	0.043	0.045	0.025	0.101	0.065	0.084	0.090	0.071	0.070	0.089	0.045	0.044
Al(VI)	0.053	0.083	0.047	0.097	0.089	0.077	0.051	0.060	0.072	0.066	0.047	0.036	0.033	0.046	0.071	0.090	0.006	–
Cr	0.009	0.001	–	0.005	0.005	0.004	0.001	0.001	0.001	0.002	–	0.002	0.003	–	0.008	0.007	0.003	–
Fe	0.846	0.901	0.851	0.808	0.834	0.823	0.813	0.751	0.780	0.919	0.883	0.836	0.868	0.917	0.834	0.836	1.077	1.099
Mn	–	0.010	–	0.005	0.006	0.004	0.004	0.007	0.003	0.010	0.006	0.007	0.006	0.003	0.012	0.012	0.015	0.013
Mg	1.107	1.009	1.117	1.048	1.041	1.065	1.109	1.157	1.102	1.004	1.060	1.129	1.102	1.032	1.072	1.051	0.900	0.893
Ca	–	–	–	0.008	0.008	0.008	0.009	0.008	0.009	0.008	0.007	0.006	0.007	0.008	–	–	0.012	0.013
Na	–	–	–	–	0.003	–	–	–	0.006	–	–	0.004	0.002	–	–	–	0.001	0.006
K	–	–	–	0.001	–	–	0.001	–	–	–	0.001	0.001	0.001	–	–	–	–	–
X_{Mg}	0.568	0.528	0.567	0.565	0.555	0.564	0.577	0.606	0.585	0.522	0.546	0.575	0.560	0.531	0.562	0.557	0.455	0.448

Table 3. Composition (wt %) of garnet from granulites of the Bryansk block, Voronezh crystalline massif

Component	5809/11						5809/4					
	large grain						grain of intermediate size				small grain	
	core			margin, near			core	margin, near *Opx*	margin, near *Pl*	margin, near *Bt*	core	margin, near *Bt*
				Opx	*Pl*	*Bt*						
	19	20	21	22	23	24	25	26	27	28	29	30
SiO_2	38.57	38.87	38.77	38.56	38.90	38.33	38.06	38.61	38.90	38.37	38.06	38.38
TiO_2	–	–	–	–	–	–	0.02	0.05	0.03	0.06	0.03	0.10
Al_2O_3	22.06	21.87	22.00	21.97	21.87	21.80	21.86	20.83	20.20	21.57	21.68	21.86
Cr_2O_3	–	–	–	–	–	–	0.13	–	0.10	0.08	0.07	0.06
FeO	29.54	28.77	29.32	30.57	29.93	31.09	29.66	29.69	30.11	30.55	29.86	29.39
MnO	0.54	0.69	0.63	0.62	0.60	0.59	0.73	0.77	0.68	0.61	0.82	0.70
MgO	7.32	7.84	7.45	6.30	7.32	6.34	7.49	7.41	7.35	6.54	6.72	6.52
CaO	2.01	2.02	1.90	2.08	2.07	1.90	1.76	2.02	1.92	2.04	1.84	2.13
Total	100.04	100.06	100.07	100.10	100.69	100.05	99.71	99.38	99.31	99.82	99.08	99.05
Alm	0.646	0.625	0.642	0.678	0.647	0.684	0.645	0.642	0.649	0.672	0.663	0.661
Sps	0.012	0.015	0.014	0.014	0.013	0.013	0.016	0.017	0.015	0.014	0.018	0.016
Prp	0.286	0.304	0.291	0.249	0.282	0.249	0.290	0.286	0.283	0.257	0.266	0.261
Grs	0.056	0.056	0.053	0.059	0.057	0.054	0.045	0.056	0.050	0.055	0.050	0.059
Uv	–	–	–	–	–	–	0.004	–	0.003	0.002	0.002	0.002
X_{Mg}	0.306	0.327	0.312	0.269	0.304	0.267	0.310	0.308	0.303	0.276	0.286	0.283

Component	5809/1											
	grain of intermediate size				small grain		inclusion in *Pl*		grain of intermediate size			inclusion in *Pl*
	core	margin, near			core	margin, near *Kfs*	core	margin, near *Pl*	core	core	margin, near *Opx*	margin, near *Pl*
		Qtz	*Bt*	*Pl*								
	31	32	33	34	35	36	37	38	39	40	41	42
SiO_2	37.06	36.79	37.46	38.14	37.96	37.28	37.82	37.65	37.69	37.54	37.72	38.09
TiO_2	0.08	0.07	0.02	0.04	0.08	0.02	0.09	0.07	0.03	0.10	0.07	0.05
Al_2O_3	21.30	21.48	21.17	21.18	21.66	21.63	21.37	21.28	21.96	21.42	21.59	21.47
Cr_2O_3	0.18	0.16	0.08	0.09	0.05	0.04	0.07	0.06	0.08	0.04	0.07	0.06
FeO	31.14	31.56	31.56	31.11	31.06	30.99	31.50	32.50	30.19	31.92	31.62	31.91
MnO	0.83	0.74	0.75	0.78	0.89	0.82	0.78	0.89	0.86	1.03	0.80	1.01
MgO	7.05	7.01	6.29	6.93	7.07	7.12	7.03	5.83	7.12	6.66	7.01	5.88
CaO	1.95	1.97	2.10	2.06	2.04	2.06	1.97	2.23	1.92	2.18	1.99	2.03
Total	99.59	99.78	99.43	100.33	100.81	99.96	100.57	100.41	99.85	100.89	100.87	100.50
Alm	0.662	0.667	0.683	0.663	0.658	0.657	0.665	0.699	0.653	0.670	0.666	0.693
Sps	0.018	0.016	0.016	0.017	0.019	0.018	0.017	0.019	0.019	0.022	0.017	0.022
Prp	0.267	0.264	0.243	0.263	0.267	0.269	0.265	0.220	0.276	0.250	0.263	0.228
Grs	0.048	0.049	0.056	0.054	0.054	0.055	0.051	0.060	0.050	0.057	0.052	0.055
Uv	0.005	0.005	0.002	0.003	0.002	0.001	0.002	0.002	0.002	0.001	0.002	0.002
X_{Mg}	0.288	0.284	0.262	0.284	0.289	0.291	0.285	0.239	0.296	0.271	0.283	0.247

Table 3. (Contd.)

Component	5809/1		5809/3								5808/4	
	inclusion in *Opx*		inclusion in *Opx*		inclusion in *Opx*				inclusion in *Pl*		large garnet	
	core	margin, near *Opx*	core	margin, near *Opx*	core			margin, near *Opx*	margin, near *Pl*	core	core	
	43	44	45	46	47	48	49	50	51	52	53	54
SiO_2	37.76	37.88	38.30	38.20	38.16	38.38	38.16	38.94	38.04	38.53	37.61	37.42
TiO_2	–	0.05	–	–	–	0.01	–	0.01	–	–	0.04	0.04
Al_2O_3	21.05	21.39	21.95	21.93	21.61	21.86	21.66	22.85	21.98	22.02	21.53	21.07
Cr_2O_3	–	0.07	0.16	0.13	0.08	0.19	0.09	0.05	0.04	–	0.01	–
FeO	32.40	31.83	30.87	30.71	30.05	30.58	30.36	29.30	29.57	29.23	33.55	33.70
MnO	0.75	0.97	0.60	0.92	1.01	0.87	0.72	1.21	0.91	0.89	0.80	0.92
MgO	6.57	6.64	6.49	6.00	6.59	6.66	6.61	6.11	6.85	7.08	5.55	5.46
CaO	2.22	1.94	1.78	2.24	1.85	1.65	1.79	1.88	1.82	2.15	1.22	1.41
Total	100.75	100.77	100.15	100.13	99.35	100.20	99.39	99.85	99.89	99.90	100.31	100.02
Alm	0.679	0.675	0.681	0.679	0.665	0.673	0.672	0.669	0.657	0.642	0.732	0.730
Sps	0.016	0.021	0.013	0.021	0.023	0.019	0.016	0.028	0.020	0.020	0.018	0.020
Prp	0.245	0.251	0.255	0.237	0.260	0.261	0.261	0.249	0.271	0.277	0.216	0.211
Grs	0.060	0.051	0.046	0.059	0.050	0.040	0.048	0.053	0.051	0.061	0.034	0.039
Uv	–	0.002	0.005	0.004	0.002	0.006	0.003	0.002	0.001	–	–	–
X_{Mg}	0.266	0.271	0.273	0.258	0.281	0.280	0.280	0.271	0.292	0.302	0.228	0.224

Component	5808/4											
	large garnet						large garnet			small garnet		
	core	margin, near					core	margin, near		core	margin, near	
		Bt	*Bt*	*Pl*	*Pl*	*Bt*		*Pl*	*Grt*		*Bt*	*Grt*
	55	56	57	58	59	60	61	62	63	64	65	66
SiO_2	37.53	37.28	37.18	37.47	37.38	37.25	37.47	37.27	37.64	37.44	37.35	37.55
TiO_2	0.03	–	0.04	0.02	0.01	0.02	0.02	–	0.03	0.04	0.05	–
Al_2O_3	21.57	21.20	21.11	20.85	21.33	21.34	21.22	20.89	21.33	21.31	21.28	21.52
Cr_2O_3	0.02	0.06	0.12	0.09	–	0.03	–	0.03	0.02	0.01	–	0.04
FeO	33.88	35.89	36.00	35.15	34.94	35.50	33.06	34.77	32.81	33.76	34.78	33.18
MnO	0.86	0.99	0.96	0.82	0.93	0.93	0.75	0.82	0.82	0.83	0.69	0.74
MgO	5.40	4.20	4.07	4.76	4.99	4.23	5.80	4.99	5.84	5.42	4.83	5.50
CaO	1.22	1.22	1.35	1.34	1.24	1.14	1.29	1.31	1.31	1.40	1.32	1.37
Total	100.51	100.84	100.83	100.50	100.82	100.44	99.61	100.13	99.80	100.21	100.30	99.90
Alm	0.737	0.781	0.783	0.761	0.754	0.781	0.722	0.753	0.717	0.733	0.760	0.729
Sps	0.019	0.022	0.021	0.018	0.020	0.021	0.017	0.018	0.018	0.018	0.015	0.016
Prp	0.210	0.163	0.158	0.184	0.192	0.166	0.226	0.193	0.228	0.210	0.188	0.216
Grs	0.034	0.032	0.034	0.034	0.034	0.031	0.036	0.034	0.036	0.039	0.037	0.037
Uv	–	0.002	0.004	0.003	–	0.001	–	0.002	0.001	–	–	0.001
X_{Mg}	0.221	0.173	0.168	0.194	0.203	0.175	0.238	0.204	0.241	0.223	0.198	0.228

Table 3. (Contd.)

Component	5808/7						
	large garnet grain with quartz and biotite inclusions						
	core, near an inclusion of				margin, near		
			Qtz	*Bt*	*Bt*	*Pl*	*Bt*
	67	68	69	70	71	72	73
SiO_2	37.23	37.12	37.37	37.26	37.38	37.31	37.09
TiO_2	0.03	0.03	0.01	0.01	–	0.03	–
Al_2O_3	21.22	21.28	21.63	21.10	21.36	21.91	20.35
Cr_2O_3	0.06	0.04	0.02	0.01	0.12	0.09	0.05
FeO	33.00	33.18	32.56	34.17	32.79	32.65	34.48
MnO	1.43	1.46	1.45	1.48	1.35	1.59	1.17
MgO	4.84	4.67	4.81	4.35	4.51	5.11	4.50
CaO	2.70	2.63	2.64	2.52	2.85	2.42	3.27
Total	100.51	100.41	100.49	100.90	100.36	100.41	100.91
Alm	0.709	0.716	0.708	0.732	0.715	0.702	0.720
Sps	0.031	0.032	0.032	0.032	0.030	0.035	0.025
Prp	0.185	0.180	0.186	0.167	0.175	0.196	0.168
Grs	0.073	0.071	0.073	0.069	0.076	0.064	0.086
Uv	0.002	0.001	0.001	–	0.004	0.003	0.001
X_{Mg}	0.207	0.201	0.208	0.185	0.197	0.218	0.189

myrmekites. Large (up to 5 mm) equant plagioclase grains in the groundmass (Samples 5809/1, 5809/4) often contain small antiperthitic inclusions of potassium feldspar. The plagioclase of Sample 5809/4 has a composition of $Ab_{44.2–50.9}An_{48.4–48.9}Or_{0.7–6.9}$ in the cores and $Ab_{46.5–48.9}An_{50.4–52.5}Or_{0.7–1.0}$ in the margins (Table 4), i.e., the mineral becomes a little more anorthitic in the margins, whatever the composition of other minerals occurring in contact with it. At contacts with large garnet grains (*Grt*-I), the anorthite content decreases from 47.0 to 45.9 (Sample 5809/11, Table 4). The plagioclase is the most calcic ($An_{55.5}$) in the matrix, away from reaction textures.

Plagioclase inclusions in orthopyroxene (Fig. 2) are devoid of apparent zoning, and their composition almost does not differ from that of large crystals. It is slightly less calcic ($An_{49.2–50.2}$) than the margins of large crystals (Table 4). The plagioclase of the plagioclase–quartz myrmekites in Sample 5809/3 (Fig. 2a) is less anorthitic ($An_{48.1}$).

Biotite. All of the rocks are relatively low in biotite (no more than 5%). The mineral has a red–brown color because of the high Ti content (5.1–6.5 wt % TiO_2), with the most titanic biotite occurring as inclusions in large garnet grains (*Grt*-I, Table 5). The distribution of Mg and Fe in biotite grains at contacts with garnet (in Sample 5809/11) shows a zonal pattern, with the margins of biotite grains (near garnet) being less magnesian (no more than 0.676) than the cores (0.693). Less magnesian biotite was detected in the groundmass (0.661) and at contacts with large garnet grains (Sample 5809/11). Biotite inclusions in newly formed garnet grains have X_{Mg} = 0.695–0.712. The most magnesian biotite (X_{Mg} = 0.724) occurs at contacts with small garnet grains (Sample 5809/4). Large biotite grains sometimes contain ilmenite inclusions and thin quartz stringers along cleavage fractures.

Quartz develops as thin rims around orthopyroxene, between garnet and orthopyroxene crystals, in plagioclase–quartz myrmekites, along cleavage planes in biotite (Fig. 2b), and small equant inclusions in large garnet grains (*Grt*-I, Fig. 3a). Quartz was encountered only in reaction textures and has never been found in the groundmass.

Ilmenite. The mineral was found in the form of small rounded grains in association with quartz and plagioclase (Sample 5809/1) and as large crystals at contacts with small garnet grains (*Grt*-II) and plagioclase (Sample 5809/4). Compositionally, it is nearly pure ilmenite with a small admixture of hematite.

Potassium feldspar occurs as large (4–5 mm) crystals (Fig. 2b) and small antiperthitic inclusions in large

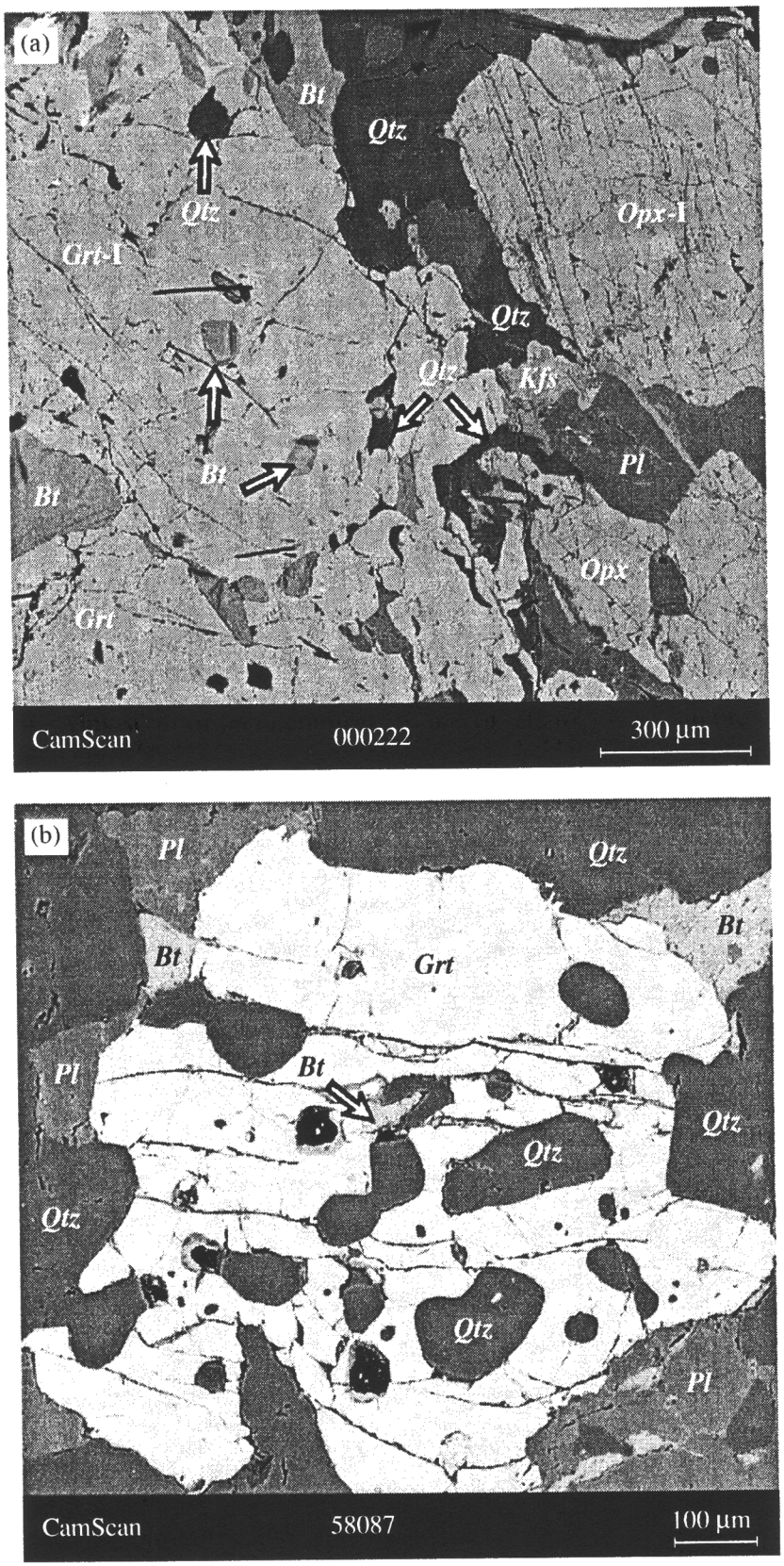

Fig. 3. Back-scattered electron images showing different garnet types from granulites of the Bryansk block.
(a) Eastern part of the block, a large garnet grain (*Grt*-I) with quartz and biotite inclusions in association with orthopyroxene (*Opx*-I), plagioclase, and quartz; Sample 5809/11.
(b) Western part of the block, an equant garnet grain with quartz and biotite inclusions; Sample 5808/7.
Images were taken on a CamScan electron microscope.

Table 4. Composition (wt %) of feldspars from granulites of the Bryansk block, Voronezh crystalline massif

Component	5809/11		5809/4					5809/1			
	Pl between *Grt* and *Opx*		large grain		perthite in *Pl*	large grain				*Kfs*	large grain
	margin, near *Grt*	core	margin, near *Opx*	core	*Pl*	core	margin, near *Grt*	core	ground-mass	core	margin, near *Opx*
	74	75	76	77	78	79	80	81	82	83	84
SiO_2	56.22	55.41	55.32	55.75	64.38	56.64	56.27	53.23	52.80	61.94	61.09
Al_2O_3	27.54	28.27	26.78	24.67	17.48	25.68	25.72	28.93	29.76	19.02	24.47
CaO	9.75	9.89	10.89	11.68	0.08	10.96	11.01	10.82	11.26	0.08	9.62
Na_2O	6.34	6.05	5.33	5.84	0.88	6.37	5.90	5.54	4.91	1.16	4.93
K_2O	–	0.19	0.17	1.39	16.19	0.13	0.12	0.11	0.11	16.84	0.11
Total	99.85	99.81	98.49	99.33	99.01	99.78	99.02	98.63	98.84	99.04	100.21
Ab	0.541	0.520	0.465	0.442	0.076	0.509	0.489	0.478	0.438	0.094	0.478
An	0.459	0.470	0.525	0.489	0.004	0.484	0.504	0.516	0.555	0.004	0.516
Or	–	0.010	0.010	0.069	0.920	0.007	0.007	0.006	0.007	0.902	0.006

Component	5809/1						5809/3				
	large grain	inclusion in *Opx*	large grain			*Kfs*	large grain with a *Grt* inclusion			large grain	
	margin, near *Grt*	core	core	core	margin, near *Opx*	core	core	near a *Grt* inclusion	margin, near *Opx*	core	margin
	85	86	87	88	89	90	91	92	93	94	95
SiO_2	59.36	54.93	58.97	53.94	54.05	61.82	56.11	55.95	56.13	55.81	55.66
Al_2O_3	25.92	28.06	25.97	28.48	28.25	19.69	27.97	27.76	27.39	27.84	28.19
CaO	8.65	10.17	9.44	10.45	10.24	0.16	9.68	9.76	9.73	10.00	10.14
Na_2O	4.64	5.73	5.10	5.60	5.63	1.16	6.00	6.17	6.14	6.02	5.93
K_2O	0.19	0.12	0.09	0.12	0.16	16.24	0.19	0.20	–	0.19	–
Total	98.76	99.01	99.57	98.59	98.33	99.07	99.95	99.84	99.39	99.86	99.93
Ab	0.486	0.501	0.492	0.489	0.494	0.097	0.523	0.528	0.533	0.516	0.514
An	0.501	0.492	0.502	0.504	0.497	0.007	0.466	0.461	0.467	0.473	0.486
Or	0.013	0.007	0.006	0.007	0.09	0.895	0.011	0.011	–	0.011	–

Component	5809/3	5808/4						5808/7			
	Pl-Qtz symplectite	inclusion in *Grt*	large grain		large grain in the groundmass			large grain		grain in the groundmass	
			margin, near *Grt*	core	margin, near *Bt*	core	core	margin, near *Grt*	core	margin, near *Bt, Qtz*	core
	96	97	98	99	100	101	102	103	104	105	106
SiO_2	56.18	58.10	60.22	59.55	59.05	59.08	58.66	56.79	54.83	57.14	55.82
Al_2O_3	27.84	26.00	25.17	24.92	25.35	26.21	25.59	27.37	28.33	26.86	27.70
CaO	10.05	6.74	6.28	6.49	6.82	6.81	6.91	8.98	10.37	8.11	9.91
Na_2O	5.93	8.04	8.43	8.18	8.19	7.81	7.82	7.15	5.71	7.30	5.90
K_2O	–	0.28	0.07	0.22	0.16	0.18	0.09	0.10	0.13	0.17	0.13
Total	100.01	99.16	100.17	99.36	99.57	100.09	99.07	100.39	99.37	99.58	99.56
Ab	0.516	0.673	0.706	0.687	0.679	0.668	0.668	0.587	0.495	0.614	0.515
An	0.484	0.312	0.290	0.301	0.312	0.322	0.327	0.408	0.497	0.377	0.478
Or	–	0.015	0.004	0.012	0.009	0.010	0.005	0.005	0.008	0.009	0.007

Table 5. Composition (wt %) of biotite from granulites of the Bryansk block, Voronezh crystalline massif

Component	5809/11						5809/4			5809/1	
	large lath		inclusion in *Grt*		ground-mass		large grain		margin, near *Grt*	core of a large lath	inclusion in *Grt*
	core	margin, near *Grt*	core	margin, near *Grt*	core	margin, near *Grt*	core	margin, near *Grt*			
	107	108	109	110	111	112	113	114	115	116	117
SiO_2	35.71	37.70	36.16	36.40	37.65	37.86	37.87	37.64	37.90	38.23	38.68
TiO_2	6.03	6.35	6.46	6.50	6.02	5.56	5.48	5.45	5.24	5.70	5.86
Al_2O_3	13.67	15.29	16.17	15.55	14.82	15.12	16.18	16.28	16.58	13.58	13.28
Cr_2O_3	0.69	–	–	–	–	–	–	0.13	0.24	0.22	0.81
FeO	13.45	12.87	11.39	11.20	13.67	12.20	11.94	11.59	10.56	12.62	11.96
MnO	–	–	–	–	–	–	0.05	–	0.01	–	–
MgO	17.06	15.07	16.85	17.00	14.94	16.06	15.27	15.61	15.54	16.12	15.96
CaO	–	–	–	–	–	–	–	0.02	–	0.03	0.10
Na_2O	–	–	–	–	–	–	0.09	0.12	0.12	0.11	0.15
K_2O	9.62	9.73	9.49	10.02	9.83	10.08	9.00	9.22	9.07	9.93	9.14
Total	96.23	97.01	96.52	96.67	96.93	96.88	95.88	96.06	95.26	96.54	95.94
Si	2.649	2.739	2.629	2.649	2.751	2.751	2.755	2.735	2.758	2.797	2.827
Ti	0.336	0.347	0.353	0.356	0.331	0.304	0.300	0.298	0.287	0.314	0.322
Al(IV)	1.195	1.261	1.371	1.334	1.249	1.249	1.245	1.265	1.242	1.171	1.144
Al(VI)	–	0.048	0.014	–	0.027	0.046	0.142	0.129	0.179	–	–
Cr	0.040	–	–	–	–	–	–	–	–	0.013	0.047
Fe	0.834	0.782	0.692	0.682	0.835	0.741	0.726	0.704	0.642	0.772	0.731
Mn	–	–	–	–	–	–	0.003	–	0.001	–	–
Mg	1.886	1.632	1.826	1.844	1.267	1.740	1.656	1.691	1.685	1.758	1.739
Ca	–	–	–	–	–	–	–	0.002	–	0.002	0.008
Na	–	–	–	–	–	–	0.013	0.017	0.017	0.016	0.021
K	0.910	0.902	0.880	0.930	0.916	0.934	0.835	0.855	0.842	0.927	0.852
X_{Mg}	0.693	0.676	0.725	0.730	0.661	0.701	0.695	0.706	0.724	0.695	0.704

Component	5809/1		5808/4					5808/7		
	small lath		large lath		margin, inclusion in *Grt*	groundmass		inclusion in *Grt*	margin, near *Grt*	groundmass
	margin, near *Grt*	core	core	margin, near *Grt*		core	margin, near *Pl*			core
	118	119	120	121	122	123	124	125	126	127
SiO_2	38.78	38.89	36.65	36.30	36.84	37.12	36.88	37.10	38.24	37.06
TiO_2	5.13	4.46	2.45	2.92	2.03	3.10	2.90	3.69	4.13	4.72
Al_2O_3	15.38	13.89	16.71	15.60	17.14	17.01	17.16	13.88	14.63	14.84
Cr_2O_3	0.55	0.06	0.27	0.34	0.94	0.10	0.27	2.05	0.21	0.12
FeO	11.89	12.55	18.04	17.90	15.75	17.27	16.70	16.56	16.64	18.84
MnO	0.03	0.06	0.04	0.04	0.04	0.08	–	0.04	0.06	–
MgO	16.45	16.58	12.65	12.30	13.38	12.17	12.44	13.06	13.91	11.67
CaO	0.10	0.01	0.04	0.05	0.20	0.07	0.08	0.17	0.04	0.01
Na_2O	0.01	0.12	0.32	0.38	0.54	0.36	0.26	0.04	0.04	0.09
K_2O	9.52	10.17	9.30	9.22	8.94	9.65	9.75	9.21	9.57	9.72
Total	96.04	96.79	96.47	95.05	95.80	96.93	96.44	95.80	97.47	97.07
Si	2.832	2.833	2.741	2.761	2.743	2.753	2.744	2.792	2.810	2.772
Ti	0.282	0.244	0.138	0.167	0.114	0.173	0.162	0.209	0.228	0.266
Al(IV)	1.168	1.167	1.259	1.239	1.257	1.247	1.256	1.208	1.190	1.228
Al(VI)	0.001	0.026	0.214	0.159	0.247	0.240	0.249	0.023	0.077	0.080
Cr	0.032	0.003	0.016	0.020	0.055	0.006	0.016	0.122	0.012	0.007
Fe	0.729	0.765	1.128	1.139	0.981	1.071	1.039	1.042	1.023	1.179
Mn	0.002	0.004	0.003	0.003	0.003	0.005	–	0.003	0.004	–
Mg	1.791	1.801	1.410	1.395	1.485	1.345	1.380	1.465	1.524	1.301
Ca	0.008	0.001	0.003	0.004	0.016	0.006	0.006	0.014	0.003	0.001
Na	0.001	0.017	0.046	0.056	0.078	0.052	0.038	0.006	0.006	0.013
K	0.887	0.945	0.887	0.895	0.849	0.913	0.925	–	0.897	0.928
X_{Mg}	0.722	0.702	0.556	0.551	0.602	0.557	0.570	0.584	0.598	0.525

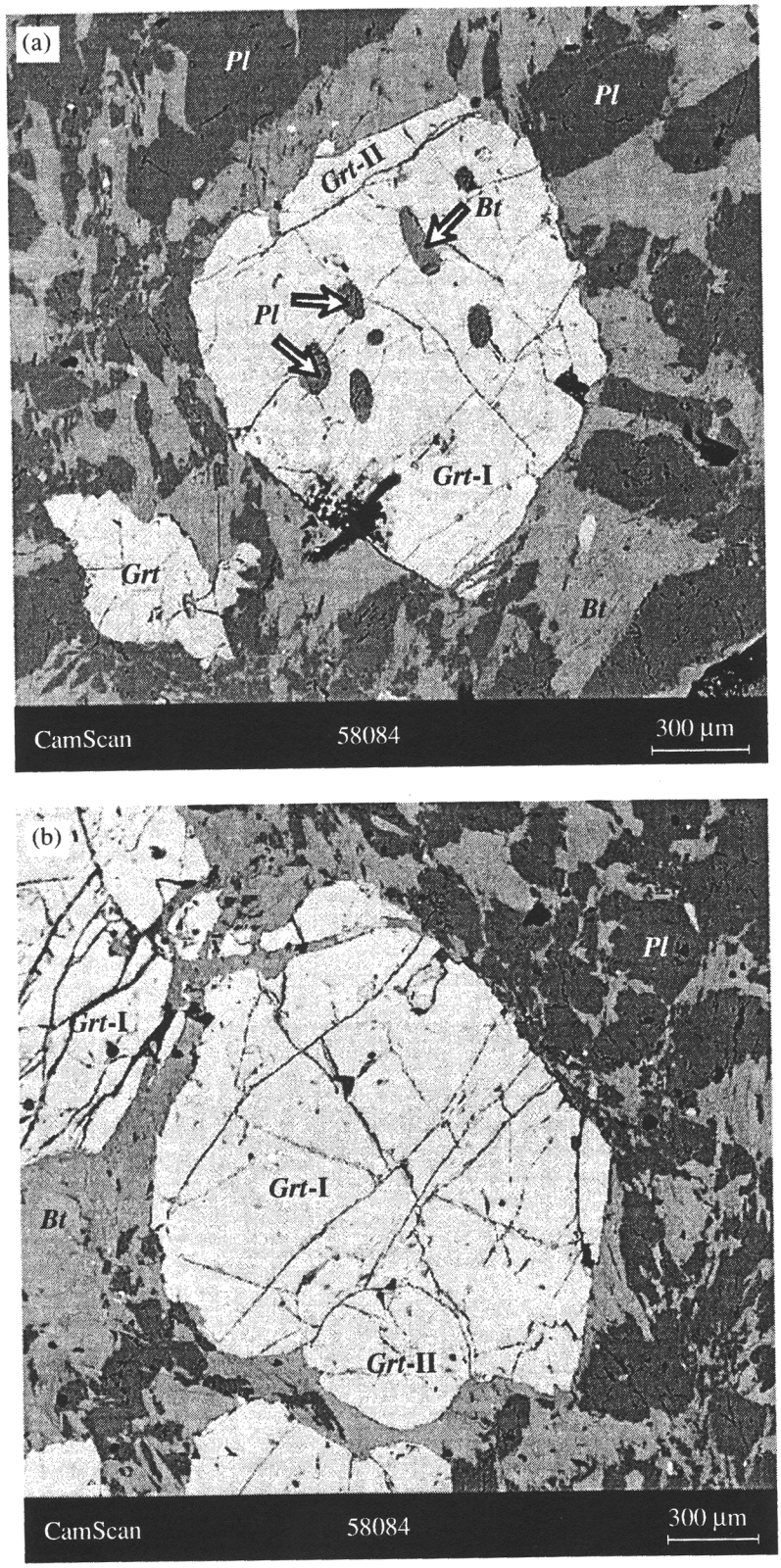

Fig. 4. Back-scattered electron images showing different garnet types from granulites in the western part of the Bryansk block.
(a) A large equant garnet grain (*Grt*-I) overgrown with a younger rim (*Grt*-II); Sample 5808/4.
(b) Aggregate of large (*Grt*-I) and smaller and younger (*Grt*-II) garnet grains; Sample 5808/4.
Images were taken on a CamScan electron microscope.

plagioclase grains. The potassium feldspar contains an insignificant admixture of the albite component.

Granulites of the Western Part of the Bryansk Block

We examined two samples of plagiogneiss from the western part of the Bryansk block (Hole 5808, Fig. 1) with an optic microscope and a microprobe. Although the rocks contain no reaction textures analogous to those described above in the granulites from the eastern portion of the block, these rocks provide useful information for comparing the *P–T* metamorphic conditions in distinct parts of the granulite complex.

The granulite of Sample 5808/4 contains the assemblage *Qtz* + *Pl* + *Grt* + *Bt* + *Sil*. The garnet occurs as large equant grains (*Grt*-I), small rounded crystals of *Grt*-II in aggregates with *Grt*-I, and rims of *Grt*-II around the earlier *Grt*-I (Figs. 4a, 4b). The newly formed garnet sometimes develops as rims or small rounded crystals in the peripheral parts of larger garnet grains. We analyzed two garnets: those devoid of inclusions, in aggregate with smaller round garnet grains and those with numerous inclusions of quartz, biotite, and plagioclase and a thin younger rim.

The large garnet (*Grt*-I) is compositionally zoned: its Mg mole fraction decreases from the core (X_{Mg} = 0.238) to rims (X_{Mg} = 0.204; Fig. 4b, Table 3). At contacts with smaller and younger garnet (*Grt*-II), its X_{Mg} = 0.241. The grossular content is nearly constant 3.4–3.6%, and the garnet is also unzoned in terms of Mn content. The equant small garnet (*Grt*-II) is more ferrous, with X_{Mg} decreasing from the core (0.223) to rims that are in contact with biotite (0.198). At contacts with the large garnet, its X_{Mg} = 0.228. The grossular and spessartine contents of the garnet slightly decrease (from 3.9 to 3.7% and from 1.7 to 1.5%, respectively) from the cores to contacts with plagioclase. The presence of two garnet generations in the rock is confirmed by their composition within a few microns from the contact. Their X_{Mg} are 0.241 and 0.228 for the large and small garnets, respectively.

Another type of large garnet (*Grt*-I) contains biotite and plagioclase inclusions and is mantled with a thin rim of homogeneous *Grt*-II (Fig. 4a). The zoning of the *Grt*-I is similar to that of the type-I garnet. Its X_{Mg} equals 0.224–0.228 in the core and decreases to 0.168–0.173 at contacts with biotite and to 0.196 at contacts with plagioclase. At contacts with the rim, its X_{Mg} = 0.221. No clear zoning in the distribution of Ca and Mn was detected. The overgrowing rim is more ferrous and less magnesian (X_{Mg} = 0.203), and its X_{Mg} decreases to 0.175 at the edge of the rim. The grossular content somewhat decreases at contacts with plagioclase (from 3.4 to 3.1%), and Mn is equally distributed over the grain.

The most calcic plagioclase ($An_{32.2}$) occurs in the groundmass of the rock, and the Ca mole fraction of this plagioclase somewhat decreases (to $An_{31.2}$) toward the margins. The plagioclase is more calcic at contacts with garnet ($An_{29.0–30.1}$) and in inclusions in garnet ($An_{31.2}$).

The biotite contains moderate amounts of Ti (2.45–3.10 wt % TiO_2) and has little varying X_{Mg} = 0.551–0.570. This interval includes the compositions of biotite both in contacts with garnet and in the groundmass. Biotite inclusions in garnet are more magnesian (X_{Mg} = 0.602) and less titanic (2.03 wt % TiO_2).

Sample 5808/7 contains the assemblage *Qtz* + *Pl* + *Grt* + *Opx* + *Bt*. The garnet occurs as large grains with embayed contours with abundant inclusions of quartz and biotite (Fig. 3b). Its X_{Mg} = 0.201–0.208 in the core and decreases to 0.185–0.197 at contacts with biotite in the matrix and biotite inclusions (Table 3). Conversely, the Mg mole fraction increases to 0.218 at contacts with plagioclase. The grossular concentration remains roughly constant (7.1–7.6%) but decreases to 6.4% at contacts with plagioclase.

The rock contains small amounts of orthopyroxene (no more than 5%), which compose elongated crystals of moderate Mg mole fraction (X_{Mg} = 0.448–0.455) and low in Al (1.11 wt % Al_2O_3), whose concentration gradually decreases toward the rim (to 0.95 wt %). Orthopyroxene grains in the groundmass never occur in contact with garnet or in reaction textures.

The plagioclase is the most calcic in the groundmass and displays notable zoning, with anorthite concentration decreasing from 47.8% in the core to 37.7% in the rim. At contacts with garnet, the plagioclase contains approximately 42% *An*.

The biotite is red–brown because of its high Ti content. The most ferrous and titanic biotite was detected in the groundmass (X_{Mg} = 0.525, 4.72 wt % TiO_2). Biotite grains at contacts with garnet and in inclusions in it are less ferrous and titanic (X_{Mg} = 0.586–0.598, 3.69–4.13 wt % TiO_2).

THERMOBAROMETRY

Granulites of the Eastern Part of the Bryansk Block

The *P–T* metamorphic conditions of the granulites with orthopyroxene, garnet, plagioclase, quartz, and, sometimes, biotite can be evaluated using the garnet–orthopyroxene (GO) and garnet–biotite (GB) thermometers and the garnet–orthopyroxene–plagioclase–quartz (GOPQ) and garnet–orthopyroxene (GOAL) barometers. However, we did not use the garnet–biotite thermometer, because the high diffusion rates of Fe and Mg in garnet–biotite pairs constrains the application of this thermometer to peak metamorphic conditions (>700°C).

P–T paths can be constructed for the granulites of the Bryansk block on the basis of the estimated *P–T* conditions during the metamorphic culmination and postculmination stage, which is reflected in reaction growth textures of garnet.

The peak metamorphic conditions were estimated on the basis of the composition of large magnesian garnet grains in their cores (*Grt*-I), large grains of aluminous orthopyroxene (*Opx*-I), and plagioclase grains in the groundmass. The temperatures and pressures of the stage of garnet growth were determined using the cores of small newly formed garnet grains (*Grt*-II and *Grt*-III) and small orthopyroxene grains (*Opx*-II), margins of plagioclase grains in the groundmass, cores and margins of very small garnets (*Grt*-IV) in plagioclase, and the margins of small orthopyroxene and plagioclase grains occurring in contact with one another.

To estimate the *P–T* conditions of metamorphism, one of these parameters should be quantified first. For this purpose, we used the thermobarometers of Aranovich and Podlesskii (1989), which make it possible to simultaneously evaluate the temperature and pressure using the composition of equilibrium garnet, orthopyroxene, and plagioclase. In estimating the *P–T* parameters, we employed the following procedure. First, GOPQ [equation (16–7)] and GO [equation (5–7)] were used to evaluate the temperature and pressure (Aranovich and Podlesskii, 1989). Analysis of these data (Table 6) indicates that the temperatures are realistic, whereas the pressures seem to be underestimated when calculated by GOPQ and overestimated when calculated by GO. Hence, the temperature of each association was taken as an average of the GOPQ and GO values (Aranovich and Podlesskii, 1989) (Table 6). Then, the pressure was estimated using the most reliable versions of GOPQ and GOAL (Table 7). All calculations were carried out with the TPF computer program (Fonarev *et al.*, 1991).

As is seen from Table 7, all of the geobarometers used in our calculations yield fairly similar values. The only exception is GOAL (Harley, 1984), which systematically underestimates pressure values by approximately 3 kbar. In constructing *P–T* paths, the pressure of each association was assumed to be equal to an average of the values obtained by the six geobarometers (Table 7). We rejected higher values obtained by GOAL (Harley, 1984). To test the compatibility of the values obtained with the geobarometers of Aranovich and Podlesskii, we calculated analogous values by several variants of the garnet–orthopyroxene geothermometer using pressure estimates for each of the associations. As can be seen from Table 8, the average temperatures determined with the six geothermometers are systematically higher than the assumed values, but the differences never exceed 28°C (averaging 17°C) and nearly coincide at higher values.

Mineral assemblages with *Grt*-I and *Opx*-I, which yield *P–T* parameters close to the maximum values, are contained only in two samples (5809/11 and 5809/4). The 5809/11 *P–T* conditions are 788–823°C and 5.3–5.5 kbar for Sample 5809/11 and 735–757°C, 4.4–4.5 kbar for Sample 5809/4 (Table 7). It is pertinent to mention that we are not sure whether the compositions corresponding to the peak *P–T* conditions are preserved in the crystal cores, and, hence, the *P–T* estimates should be regarded as the lower limit of the conditions during the metamorphic climax. The above-mentioned *P–T* estimates are consistent with analogous values obtained on magnesian marbles from the Bryansk block of the Voronezh crystalline massif (700–770°C and 5.0–5.7 kbar; Savko and Lebedev, 1996).

The estimated *P–T* conditions of the garnet growth stage are as follows: T = 673–708°C and P = 4.2–4.6 kbar for Sample 5809/4, T = 594–732°C, P = 2.8–4.0 kbar for Sample 5809/1, T = 666–742°C and P = 3.3–4.8 kbar for Sample 5809/3, and T = 665°C and P = 3.6 kbar for Sample 5809/11. In general, the *P–T* conditions of the rocks vary over the intervals 742–594°C and 4.8–2.8 kbar and compose a clear-cut linear *P–T* path (Fig. 5). The values of 793°C and 5.1 kbar, which were calculated based on compositions in the margins of large orthopyroxene grains and small grains of garnet in Sample 5809/1, are caused by the higher Fe mole fraction of the hypersthene and, perhaps, reflect the earliest cooling stage. As is seen in Fig. 5, the swarms of *P–T* points of the culmination and garnet-growth stages overlap within a common linear trend, probably because of the reequilibration of medium-sized garnet grains in Sample 5809/4 after the metamorphic peak.

Granulites of the Western Part of the Bryansk Block

The procedure of *P–T* estimates in Sample 5808/7 (which contained the *Grt–Opx–Pl–Qtz–Bt* assemblage) was analogous to that described above in application to the granulites from the eastern portion of the block. Since the rock contained no reaction textures, our estimates (based on "core–core" and "margin–margin" pairs) correspond to *P–T* conditions close to those of the metamorphic culmination and the subsequent stage. Because 80% of the garnet grain analyzed for thermobarometry is surrounded by quartz and plagioclase (Fig. 3b), no significant changes in the Fe and Mg concentrations occurred at contacts with these minerals. The Mg mole fraction of the garnet decreases only towards contacts with biotite, which occur in the groundmass and as inclusions. Because of this, the temperature of the metamorphic culmination was evaluated using both the cores and peripheral parts of the garnet at contacts with quartz and plagioclase. The temperature of the cooling stage was quantified based on the composition of garnet at contacts with biotite. Temperature that presumably corresponds to the peak values was calculated as an average of GO and GOPQ estimates (Aranovich and Podlesskii, 1989) and ranges from 795 to 845°C (Table 6). The pressure during this stage was calculated as an average of estimates obtained by five geobarometers (Table 9) and ranges from 4.4 to 5.0 kbar. Because of the low Al_2O_3 concentration in the orthopyroxene, the geobarometers based on the solubility of this component in orthopyroxene in assemblage with garnet (Harley, 1984; Harley and

Table 6. Compositional parameters of minerals from granulites of the Bryansk block and the estimated temperatures of mineral equilibria

Sample number	Assemblage and numbers of analyses (see Tables 2–4)	*Grt*		*Opx*		*Pl*	*T*, °C, thermometers of Aranovich and Podlesskii (1989)		
		X_{Mg}	*Grs*	X_{Mg}	X_{Al}	*An*	GO	GOPO	T_{calc}
5809/11	*Grt*(20)–*Opx*(1)–*Pl*(75)–*Qtz*	0.327	0.056	0.568	0.145	0.470	809	767	788
5809/11	*Grt*(21)–*Opx*(2)–*Pl*(75)–*Qtz*	0.312	0.053	0.528	0.177	0.470	842	804	823
5809/11	*Grt*(22)–*Opx*(3)–*Pl*(74)–*Qtz*	0.269	0.059	0.567	0.123	0.459	678	652	665
5809/4	*Grt*(25)–*Opx*(5)–*Pl*(79)–*Qtz*	0.310	0.045	0.555	0.161	0.484	773	740	757
5809/4	*Grt*(25)–*Opx*(4)–*Pl*(79)–*Qtz*	0.310	0.045	0.565	0.160	0.484	750	720	735
5809/4	*Grt*(29)–*Opx*(25)–*Pl*(76)–*Qtz*	0.286	0.050	0.577	0.094	0.525	713	668	691
5809/4	*Grt*(30)–*Opx*(6)–*Pl*(76)–*Qtz*	0.283	0.059	0.564	0.131	0.525	714	686	700
5809/4	*Grt*(26)–*Opx*(8)–*Pl*(80)–*Qtz*	0.308	0.056	0.606	0.105	0.504	691	654	673
5809/4	*Grt*(27)–*Opx*(9)–*Pl*(80)–*Qtz*	0.303	0.050	0.585	0.097	0.504	731	684	708
5809/1	*Grt*(44)–*Opx*(11)–*Pl*(86)–*Qtz*	0.271	0.051	0.546	0.112	0.492	735	694	715
5809/1	*Grt*(43)–*Opx*(10)–*Pl*(86)–*Qtz*	0.266	0.060	0.522	0.167	0.492	743	720	732
5809/1	*Grt*(31)–*Opx*(12)–*Pl*(82)–*Qtz*	0.288	0.048	0.573	0.120	0.555	704	669	687
5809/1	*Grt*(40)–*Opx*(13)–*Pl*(85)–*Qtz*	0.271	0.057	0.560	0.123	0.501	702	671	687
5809/1	*Grt*(35)–*Opx*(14)–*Pl*(84)–*Qtz*	0.289	0.054	0.530	0.117	0.516	819	766	793
5809/1	*Grt*(38)–*Opx*(12)–*Pl*(88)–*Qtz*	0.239	0.060	0.573	0.120	0.504	602	585	594
5809/1	*Grt*(42)–*Opx*(13)–*Pl*(89)–*Qtz*	0.247	0.055	0.560	0.123	0.497	644	621	633
5809/3	*Grt*(45)–*Opx*(15)–*Pl*(91)–*Qtz*	0.273	0.046	0.562	0.141	0.466	678	654	666
5809/3	*Grt*(52)–*Opx*(15)–*Pl*(95)–*Qtz*	0.302	0.061	0.562	0.141	0.486	757	726	742
5809/3	*Grt*(51)–*Opx*(15)–*Pl*(96)–*Qtz*	0.292	0.051	0.562	0.141	0.486	727	696	712
5808/7	*Grt*(67)–*Opx*(17)–*Pl*(106)–*Qtz*	0.207	0.073	0.455	0.051	0.478	834	756	795
5808/7	*Grt*(70)–*Opx*(18)–*Pl*(103)–*Qtz*	0.185	0.069	0.448	0.044	0.407	784	710	747
5808/7	*Grt*(69)–*Opx*(17)–*Pl*(104)–*Qtz*	0.208	0.073	0.455	0.051	0.497	838	758	798
5808/7	*Grt*(72)–*Opx*(18)–*Pl*(103)–*Qtz*	0.218	0.064	0.448	0.044	0.407	895	794	845
5808/7	*Grt*(73)–*Opx*(18)–*Pl*(105)–*Qtz*	0.189	0.086	0.448	0.044	0.377	806	736	771

Note: GO is the garnet–orthopyroxene thermobarometer, GOPQ is the garnet–orthopyroxene–plagioclase–quartz thermobarometer.

Green, 1982) yield unrealistically high values (11–18 kbar), which were rejected. The temperature and pressure of the postculmination stage were estimated at 747–771°C and 4.0–4.2 kbar. Figure 6 demonstrates that these values compose a linear (but relatively short) trend with a relatively small difference between the *P–T* conditions of the metamorphic peak and the subsequent stage.

Sample 5808/4 contains the *Grt–Pl–Sil–Qtz–Bt* assemblage. It cannot be used to estimate the temperatures near the metamorphic peak: the garnet–biotite thermometer gives underestimated temperature values because of a change in the biotite composition under the effect of later unequilibrated Fe–Mg exchange reactions with the garnet, and this geothermometer can be used to estimated the temperature during the postculmination stage. The pressure for Sample 5808/4 was evaluated by the *Grt–Pl–Sil–Qtz* geobarometer. It is worth noting that this barometer is highly sensitive to temperature, and, thus, this parameter should be evaluated particularly carefully. Biotite–garnet thermometry is little dependent on pressure: within the *P–T* field of metamorphic processes, a pressure change as large as 1 kbar will cause a temperature change of no more than 4°C. The *P–T* estimates obtained for the postculmination stage are 607–660°C and 2.9–4.0 kbar (Tables 10, 11, Fig. 6).

If the temperature of the culmination stage is assumed to be 800°C (this value was calculated by the *Grt–Opx–Pl–Qtz* thermometer for Sample 5808/7, which was collected from the core of the same hole as Sample 5808/4), the area of peak metamorphic parameters in the *P–T* plot of Fig. 6 should be $T = 800 \pm 20$°C and $P = 5.4$–6 kbar.

Table 7. Estimated pressures of mineral equilibria in granulites from the eastern part of the Bryansk block

Sample number	Assemblage and numbers of analyses (see Tables 2–4)	T, °C	Geobarometers							P_{av}, kbar
			GOPQ					GO		
			PN	PC	GF	E	B	HG	H	
5809/11	*Grt*(20)–*Opx*(1)–*Pl*(75)–*Qtz*	788	5.8	5.0	5.1	5.3	5.0	6.5	9.3	5.4
5809/11	*Grt*(21)–*Opx*(2)–*Pl*(75)–*Qtz*	823	6.0	5.3	5.0	5.5	4.8	5.6	8.1	5.3
5809/11	*Grt*(22)–*Opx*(3)–*Pl*(74)–*Qtz*	665	4.0	3.8	3.1	3.5	4.5	2.6	5.6	3.6
5809/4	*Grt*(25)–*Opx*(5)–*Pl*(79)–*Qtz*	757	5.1	4.4	4.1	4.6	4.2	4.3	7.5	4.5
5809/4	*Grt*(25)–*Opx*(4)–*Pl*(79)–*Qtz*	735	5.1	4.3	4.1	4.6	4.3	4.2	6.9	4.4
5809/4	*Grt*(29)–*Opx*(7)–*Pl*(76)–*Qtz*	691	4.0	3.5	3.1	3.5	4.1	6.1	9.3	4.1
5809/4	*Grt*(30)–*Opx*(6)–*Pl*(76)–*Qtz*	700	4.8	4.4	3.7	4.3	4.5	3.6	6.4	4.2
5809/4	*Grt*(26)–*Opx*(8)–*Pl*(80)–*Qtz*	673	4.5	3.9	3.5	4.1	4.5	5.1	8.6	4.2
5809/4	*Grt*(27)–*Opx*(9)–*Pl*(80)–*Qtz*	708	4.6	3.7	3.6	4.1	4.4	6.8	10.0	4.6
5809/1	*Grt*(44)–*Opx*(11)–*Pl*(86)–*Qtz*	715	4.1	3.8	3.4	3.6	4.2	5.1	7.8	4.0
5809/1	*Grt*(31)–*Opx*(12)–*Pl*(82)–*Qtz*	687	3.9	3.3	3.2	3.4	4.0	3.9	7.2	3.6
5809/1	*Grt*(40)–*Opx*(13)–*Pl*(85)–*Qtz*	687	4.1	3.9	3.5	3.6	4.3	3.4	6.2	3.8
5809/1	*Grt*(35)–*Opx*(14)–*Pl*(84)–*Qtz*	793	4.9	4.5	4.3	4.4	4.5	7.7	10.0	5.1
5809/1	*Grt*(38)–*Opx*(12)–*Pl*(88)–*Qtz*	594	3.1	3.2	1.8	2.6	3.9	–	3.0	2.9
5809/1	*Grt*(42)–*Opx*(13)–*Pl*(89)–*Qtz*	633	3.2	3.2	2.2	2.8	3.9	1.2	4.1	2.8
5809/1	*Grt*(43)–*Opx*(10)–*Pl*(86)–*Qtz*	732	4.7	4.6	4.0	4.2	4.4	2.3	4.5	4.1
5809/3	*Grt*(45)–*Opx*(15)–*Pl*(91)–*Qtz*	666	4.0	3.6	2.8	3.5	3.9	1.7	5.1	3.3
5809/3	*Grt*(52)–*Opx*(15)–*Pl*(95)–*Qtz*	742	5.2	4.8	4.5	4.7	4.8	4.7	7.4	4.8
5809/3	*Grt*(51)–*Opx*(15)–*Pl*(96)–*Qtz*	712	4.4	3.9	3.5	3.9	4.2	3.6	6.7	3.9

Note: The following abbreviations are used in Tables 7 and 9: garnet–orthopyroxene–plagioclase–quartz (GOPQ) and garnet–orthopyroxene (GO) geobarometers: PN—Perkins and Newton (1981), PC—Perkins and Chipera (1982), GF—Grafchikov and Fonarev (1991), E—Eckert *et al.* (1991), B—Bhattacharya (1984), HG—Harley and Green (1982), and H—Harley (1984).

P–T PATHS

The *P–T* estimates obtained on the four granulite samples from the eastern portion of the Bryansk block make it possible to draw a generalized retrograde *P–T* path for the evolution of the granulites from a maximum temperature of 800–850°C and a pressure of about 5.5 kbar. The minimum values, which correspond to the closure of the system and termination of metamorphic reactions, are ~600°C and 3 kbar. As can be seen in Fig. 7, the *P–T* trajectories of individual samples pass not far from one another but have different initial and final parameters. This indicates that the methods selected to determine the *P–T* conditions of the granulites are quite reliable, and the differences between the initial and final values are explained by the absence of mineral assemblages of the metamorphic culmination in some of our samples (Samples 5809/1, 5809/3) or the lack of reaction textures corresponding to the *P–T* conditions of the lower part of the path in others (in Sample 5809/11). Hence, our generalized *P–T* path (Fig. 7) should correspond to the retrograde evolution of the granulites in the eastern part of the Bryansk block. The path corresponds to a geothermal gradient of 1.2 kbar/100°C (20°C/km) and passes between the typical *P–T* trajectories for isothermal decompression (ITD) and isobaric cooling (IBC). Based on analysis of approximately ninety granulite complexes, Harley (1989) arrived at the conclusion that most ITD trajectories correspond to gradients in the range from 2.4 to 3.0 kbar/100°C, whereas IBC trajectories usually have gradients of 0.3–0.5 kbar/100°C.

The *P–T* path constructed for the two samples from the western part of the Bryansk block (Fig. 8, large arrow) is situated close to the *P–T* path for the eastern part of the block and has maximum values of $T = 850$°C and $P = 6$ kbar and minimum values of $T = 600$°C and $P = 2.9$ kbar, which are similar to the corresponding values for the eastern part of the block.

It follows that the *P–T* trajectories of granulites in the Bryansk block answer to a geothermal gradient of 20°C/km, which is an average of values proposed by different researchers for the relatively stable Archean crust (England and Bickle, 1984; Nisbett, 1984). This means that the granulites were uplifted for approximately 10 km, and their temperature thereby decreased by 220°C. The mineral assemblages of the rock provide no information on their further evolution, because the system became closed at temperatures below 600°C.

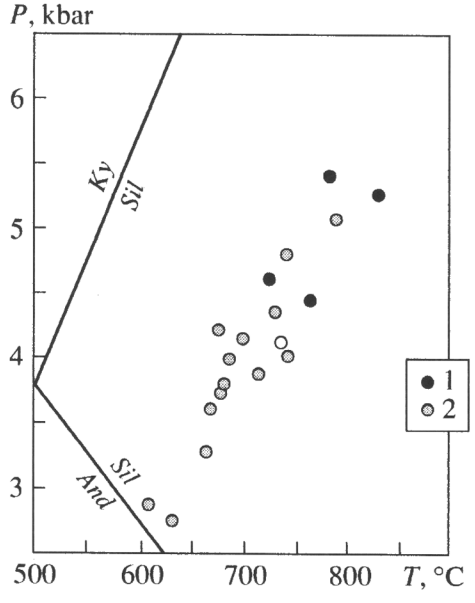

Fig. 5. Estimated *P–T* conditions of different metamorphic stages in the eastern part of the Bryansk block.
(1, 2) *P–T* parameters: (1) culmination stage, (2) postculmination stage.

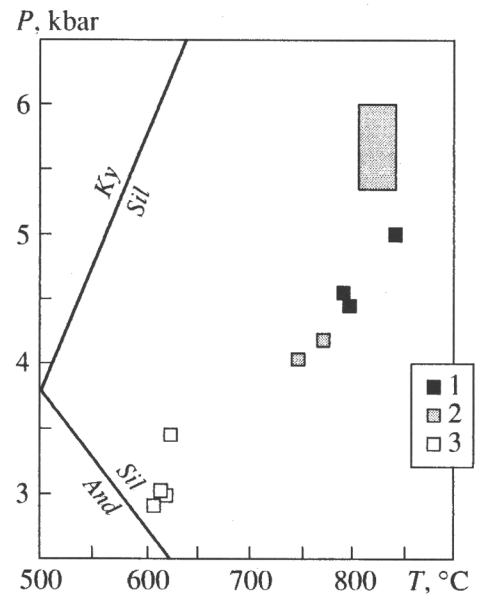

Fig. 6. Estimated *P–T* conditions of different metamorphic stages in the western part of the Bryansk block.
(*1*, *2*) *P–T* parameters: (*1*) culmination stage (Sample 5808/7), (*2*) postculmination stage (Sample 5808/7), and (*3*) postculmination stage (Sample 5808/4). The shaded rectangle presents the peak *P–T* conditions determined in Sample 5808/4.

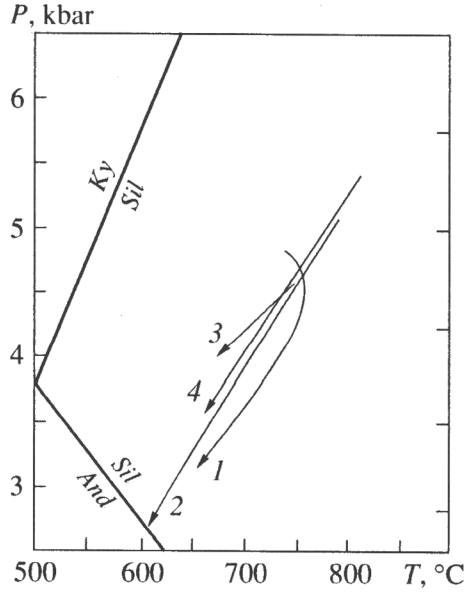

Fig. 7. Retrograde *P–T* paths for granulites in the eastern part of the Bryansk block.
(*1*) Sample 5809/3; (*2*) Sample 5809/1; (*3*) Sample 5809/4; and (*4*) Sample 5809/11.

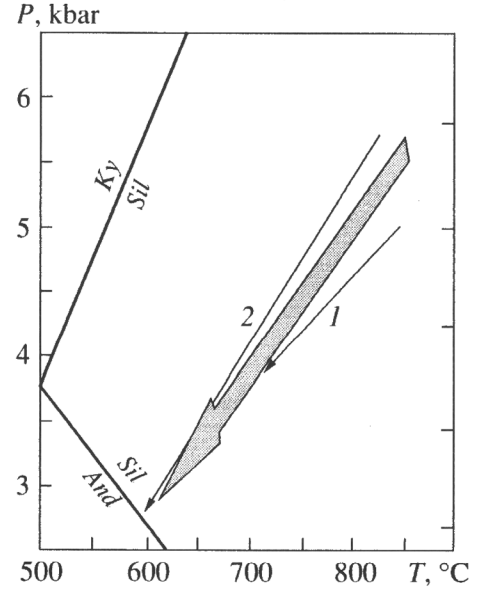

Fig. 8. Retrograde *P–T* paths for granulites in the western part of the Bryansk block.
(*1*) Sample 5808/7; (*2*) Sample 5808/4. The large area shows a generalized retrograde path.

TECTONO-THERMAL EVOLUTION OF GRANULITES IN THE BRYANSK BLOCK

The absence of isotopic estimates of the metamorphic age hampers our capability of interpreting petrological data. The general character of the prograde metamorphism (the absence of zoning and gently dipping structures, such as depressions and uplifts with dips at angles of 5–20°) suggests that the process occurred in the Early Archean. Because Early Proterozoic metamorphic complexes are normally zoned, their structures are characterized by steep dips, even the maximum *P–T* parameters of these processes did not attain the granulite facies, and the rocks of the Late Archean greenstone belts are metamorphosed to the greenschist and epidote amphibolite facies. According

Table 8. Comparison of the assumed temperatures and respective temperatures calculated by different geothermometers

Sample number	Assemblage and numbers of analyses (see Tables 2–4)	P, kbar	Geothermometers						T_{av}, °C	$\Delta T = T_{as} - T_{av}$
			H	SB	AK	LG	PL	B		
5809/11	*Grt*(20)–*Opx*(1)–*Pl*(75)–*Qtz*	5.4	731	812	777	826	768	760	779	+9
5809/11	*Grt*(21)–*Opx*(2)–*Pl*(75)–*Qtz*	5.3	775	880	813	872	799	801	823	0
5809/11	*Grt*(22)–*Opx*(3)–*Pl*(74)–*Qtz*	3.6	597	629	661	678	632	651	641	+24
5809/4	*Grt*(25)–*Opx*(5)–*Pl*(79)–*Qtz*	4.5	708	780	750	798	733	740	752	+5
5809/4	*Grt*(25)–*Opx*(4)–*Pl*(79)–*Qtz*	4.4	690	753	732	778	714	724	732	+3
5809/4	*Grt*(29)–*Opx*(7)–*Pl*(76)–*Qtz*	4.1	617	653	681	701	662	664	663	+28
5809/4	*Grt*(30)–*Opx*(6)–*Pl*(76)–*Qtz*	4.2	636	681	698	723	669	683	682	+18
5809/4	*Grt*(26)–*Opx*(8)–*Pl*(80)–*Qtz*	4.2	612	644	665	695	658	657	655	+18
5809/4	*Grt*(27)–*Opx*(9)–*Pl*(80)–*Qtz*	4.6	639	681	698	723	685	682	685	+23
5809/1	*Grt*(44)–*Opx*(11)–*Pl*(86)–*Qtz*	4.0	638	685	706	721	676	686	685	+26
5809/1	*Grt*(43)–*Opx*(10)–*Pl*(86)–*Qtz*	4.1	669	730	730	760	690	715	716	+16
5809/1	*Grt*(31)–*Opx*(12)–*Pl*(82)–*Qtz*	3.6	621	659	680	705	660	667	665	+22
5809/1	*Grt*(40)–*Opx*(13)–*Pl*(85)–*Qtz*	3.8	616	653	682	704	653	666	662	+25
5809/1	*Grt*(35)–*Opx*(14)–*Pl*(84)–*Qtz*	5.1	714	791	778	809	753	750	766	+27
5809/1	*Grt*(38)–*Opx*(12)–*Pl*(88)–*Qtz*	2.9	529	540	598	607	564	595	572	+22
5809/1	*Grt*(42)–*Opx*(13)–*Pl*(89)–*Qtz*	2.8	563	584	632	645	595	622	607	+26
5809/3	*Grt*(45)–*Opx*(15)–*Pl*(91)–*Qtz*	3.3	608	643	666	687	635	659	650	+16
5809/3	*Grt*(52)–*Opx*(15)–*Pl*(95)–*Qtz*	4.8	681	741	735	775	713	719	727	+15
5809/3	*Grt*(51)–*Opx*(15)–*Pl*(96)–*Qtz*	3.9	653	702	706	742	682	694	697	+15

Note: T_{as}—assumed temperature, T_{av}—average temperature calculated by the thermometers of: H—Harley (1984), SB—Sen and Bhattacharya (1984), AK—Aranovich and Kosyakova (1987), LG—Lee and Ganguly (1988), PL—Perchuk and Lavrent'eva (1990), and B—Bhattacharya (1984).

Table 9. Estimated pressures (kbar) of mineral equilibria in granulites from the western part of the Bryansk block (Sample 5808/7)

Assemblage and numbers of analyses (see Tables 2–4)	T, °C	Geobarometers					P_{av}, kbar
		GOPQ					
		PN	PC	GF	E	B	
Grt(67)–*Opx*(17)–*Pl*(106)–*Qtz*	795	4.4	5.1	4.4	3.9	5.1	4.6
Grt(70)–*Opx*(18)–*Pl*(103)–*Qtz*	747	3.6	4.7	3.8	3.2	4.9	4.0
Grt(69)–*Opx*(17)–*Pl*(104)–*Qtz*	798	4.3	5.0	4.2	3.8	4.9	4.4
Grt(72)–*Opx*(18)–*Pl*(103)–*Qtz*	845	5.0	5.4	4.8	4.5	5.4	5.0
Grt(73)–*Opx*(18)–*Pl*(105)–*Qtz*	771	3.7	4.9	4.1	3.2	5.1	4.2

to Novikova and Shchipanskii (1988), Early Proterozoic sedimentation in basins with iron mineralization of the Kursk Magnetic Anomaly occurred on the granulite–gneiss basement of blocks cratonized in Archean time and devoid of the granite layer. Metamorphic evolution had a similar character throughout the Bryansk block, a fact corroborated by the similarity of the P–T trajectories constructed for samples from different parts of the block (Fig. 1).

The modern thickness of the crust in the Bryansk block is 38–40 km, as was determined during deep seismic sounding along the Zheleznogorsk–Bryansk profile, and, in contrast to other structures (including Archean ones) of the Voronezh crystalline massif, the block has no discontinuity that is the first to occur below the surface of the crystalline basement, corresponds to the granite layer, and is characterized by velocities of 6.3–6.7 km/s (Golionko and Krestin, 1975). Within the Voronezh crystalline massif, the

Table 10. Estimated temperatures of mineral equilibria in granulites (Sample 5808/4) of the postculmination stage at a pressure of 4 kbar, data of the garnet–biotite thermometer, western part of the Bryansk block

Assemblage and numbers of analyses (see Tables 3, 5)	Garnet–biotite thermometer						T_{av}, °C
	FS	HS	HL	P	LP	PG	
Grt(62)–*Pl*(100)–*Qtz*–(*Sil*)–*Bt*(124)	595	618	595	591	609	636	607
Grt(64)–*Pl*(102)–*Qtz*–(*Sil*)–*Bt*(123)	660	684	637	625	647	706	660
Grt(65)–*Pl*(98)–*Qtz*–(*Sil*)–*Bt*(121)	613	636	606	601	621	653	622
Grt(59)–*Pl*(99)–*Qtz*–(*Sil*)–*Bt*(120)	616	637	608	602	621	657	619
Grt(58)–*Pl*(100)–*Qtz*–(*Sil*)–*Bt*(121)	603	626	600	596	615	645	614

Note: Geothermometers: FS—Ferry and Spear (1978), HS—Hodges and Spear (1982), HL—Holdaway and Lee (1978), P—Perchuk (1989), FS—Lavrent'eva and Perchuk (1984), and PG—Pigage and Greenwood (1982).

Table 11. Estimated pressures (kbar) of mineral equilibria in granulites from the western part of the Bryansk block (Sample 5808/4)

Assemblage and numbers of analyses (see Tables 3, 4)	T, °C	Geobarometers					P_{av}, kbar
		GASP					
		NH	GS	BS	KN	AP	
Grt(62)–*Pl*(100)–*Qtz*–(*Sil*)	607	3.3	2.8	3.3	4.1	1.0	2.9
Grt(64)–*Pl*(102)–*Qtz*–(*Sil*)	660	4.4	3.8	4.3	5.2	2.2	4.0
Grt(65)–*Pl*(98)–*Qtz*–(*Sil*)	622	3.9	3.3	3.9	4.7	1.5	3.5
Grt(59)–*Pl*(99)–*Qtz*–(*Sil*)	619	3.4	2.8	3.4	4.3	1.1	3.0
Grt(58)–*Pl*(100)–*Qtz*–(*Sil*)	614	3.5	2.9	3.4	4.3	1.1	3.1

Note: Garnet–Al silicate–plagioclase–quartz (GASP) geobarometer: NH—Newton and Haselton (1984), GS—Ganguly and Saxena (1984), BS—Bhattacharya and Sen (1984), KN—Koziol and Newton (1988), and AP—Aranovich and Podlesskii (1989).

thickness of the granite layer is commonly 14–27 km (Nadezhka *et al.*, 1989). All rocks (except marbles and migmatites) exposed at the Precambrian erosion surface within the Bryansk block have relatively high densities (2.8–3.0 g/cm^3), which correspond to the "diorite layer" with velocities (v_p) of 7.0–7.1 km/s. This layer was interpreted as a stratum of mafic granulites (Golionko *et al.*, 1973; Tarkov, 1974) with a thickness of 5–7 km (Nozhkin and Krestin, 1984). Hence, the Bryansk block is characterized by a "thick" lithosphere.

As follows from the data presented above, the thickness of rocks eroded within the Bryansk block was 14–27 km. Our petrological data suggest that the granulites were uplifted for 10 km, which is also confirmed by thermobarometric data. The remaining 10–12 km of the uplift magnitude corresponded to the transportation of the rocks to the Precambrian surface and are not reflected in the mineral assemblages because of kinetic factors (the closure of the system at temperatures of about 600°C). Hence, the granulites currently observable at the Precambrian erosion surface of the Bryansk block were exhumed from depths of approximately 20–22 km, which is consistent with seimologic results.

The data and considerations presented above suggest the following sequence of geologic events within the Bryansk block in Archean time:

(1) subsidence of the heavy crust of the Bryansk block relative to lighter sialic segments and the accumulation of a sedimentary sequence (pelites, carbonates, and ferrous rocks);

(2) collision and accompanying magmatism, tectonic thickening of the crust, prograde metamorphism, and subsequent isobaric cooling; and

(3) erosion of the thickened crust and the exhumation of the granulite complex.

This sequence of geologic events is consistent with the geodynamic evolution model proposed by Chernyshov *et al.* (1997) for the Voronezh crystalline massif. According to the model, the Early Archean evolutionary cycle ended with collision (at 3.0 Ga).

The prograde metamorphism (with peak temperatures higher than 800°C) proceeded within the andalusite–sillimanite stability field, as follows from the relatively low pressures (no higher than 6 kbar) during the culmination stage and the absence of kyanite relics. According to England and Thompson (1984), *P–T* trajectories that resulted from collision-related crust thickening cannot attain temperatures higher than 800°C if there is no additional heat source. As can be

seen in Fig. 1, granitic magmatism was developed within the Bryansk block much more widely than mafic magmatism. This points to a significant melting degree during the sinking of the lower crust as a result of its collisional thickening and a high heat flux. The resultant magma volumes were intruded into the overlying sedimentary rocks with a relatively high velocity, which was a few orders of magnitude higher than the rates of uplift and erosion (Thompson, 1989). The magma served as an additional heat source. After the metamorphic peak, the rocks were isobarically cooled, a process reflected in the development of reaction textures of garnet growth. In environments of the tectonic thickening of the relatively homogeneous crust and accompanying magmatic activity, the isobaric cooling of the rocks begins immediately after the metamorphic culmination (England and Richardson, 1977; Ellis, 1987). The cooling was caused by the conductive relaxation of the heat flux as a consequence of the cooling of syntectonic plutons, a process whose rate was several orders of magnitude higher than the erosion rate. This "magmatic accretion" mechanism was often invoked to account for the nature of IBC trajectories (Wells, 1980; Bohlen, 1991; etc.).

The different uplift magnitudes of the Bryansk block and neighboring structures resulted in the isostatic compensation of the thickened crust and the erosion of the Archean "mountains." The erosion was probably accompanied by crustal extension. This is confirmed by the origin of gently dipping fold structures in the Bryansk granulites, a process that could result from the extension of thickened crust (Sandiford and Powell, 1986; Sandiford, 1989).

CONCLUSION

This paper presents petrological data on an extensive granulite terrane, the Bryansk block of the Voronezh crystalline massif. The granulites of intermediate composition contain reaction textures of garnet growth, which suggest that the rocks experienced isobaric cooling after the metamorphic culmination. The metamorphic conditions, which were determined for the stage close to the culmination by mineralogical thermobarometry, were approximately 850°C and 5.5–6 kbar. The minimum *P–T* parameters were estimated by the composition of coexisting minerals at 600°C and 3.0 kbar. The *P–T* paths correspond to a geothermal gradient of 1.2 kbar/100°C (20°C/km) and pass between the typical ITD and IBC trajectories. Mineral assemblages provide information on the uplift of the granulites for approximately 10 km and a simultaneous temperature decrease by 220°C. The *P–T* paths based on thermobarometric data on granulites from the western and eastern portions of the area are very similar, a fact suggesting that the metamorphic evolution of the rocks was the same throughout the Bryansk block.

The granulite metamorphism was caused by the tectonic thickening of the Archean crust as a result of collision and the simultaneous origin and ascent of granitic melts. Immediately after the metamorphic culmination, the rocks underwent nearly isobaric cooling as a consequence of the cooling of syntectonic plutons. The subsequent erosion brought the rocks to the Precambrian erosion surface.

ACKNOWLEDGMENTS

This study was financially supported by Grant MPI (MGGA) NICh–823 on fundamental research in geology, geological prospecting, and surveying.

REFERENCES

Aranovich, L.Ya. and Kosyakova, N.A., Garnet–Orthopyroxene Geothermobarometer: Thermodynamics and Applications, *Geokhimiya*, 1987, no. 10, pp. 1363–1367.

Aranovich, L.Ya. and Podlesskii, K.K., Geothermobarometry of High-Grade Metapelites: Simultaneously Operating Reactions, *Evolution of Metamorphic Belts*, Daly, J.S., Cliff, R.A., and Yardley, B.W.D., Eds, *Geol. Soc. Spec. Publ.* (London), 1989, no. 43, pp. 45–61.

Bhattacharya, A. and Sen, S.K., Energetics of Hydration of Cordierite and Water Barometry in Cordierite Granulites, *Contrib. Mineral. Petrol.*, 1985, vol. 89, no. 4, pp. 370–378.

Bhattacharya, A., Krishnakumar, K.R., Raith, M., and Sen, S.K., An Improved Set of a–X Parameters for Fe–Mg–Ca Garnets and Refinements of the Orthopyroxene–Garnet Thermometer and the Orthopyroxene–Garnet–Plagioclase–Quartz Barometer, *J. Petrol.*, 1991, vol. 32, no. 3, pp. 629–656.

Bohlen, S.R., On the Formation of Granulites, *J. Metamorph. Geol.*, 1991, vol. 9, no. 3, pp. 223–229.

Chernyshov, N.M., Nenakhov, V.M., Lebedev, I.P., and Strik, Yu.N., A Model for the Geodynamic Evolution of the Voronezh Massif in the Early Precambrian, *Geotektonika*, 1997, no. 3, pp. 21–30.

Eckert, J.O., Newton, R.C., and Kleppa, O.J., The ΔH of Reaction and Recalibration of Garnet–Pyroxene–Plagioclase–Quartz Geobarometers in the CMAS System by Solution Calorimetry, *Am. Mineral.*, 1991, vol. 76, no. 1/2, pp. 148–160.

Ellis, D.J., Origin and Evolution of Granulites in Normal and Thickened Crusts, *Geology*, 1987, vol. 15, pp. 167–170.

England, P.C. and Bickle, M., Continental Thermal and Tectonic Regimes during the Archean, *J. Geol.*, 1984, vol. 92, pp. 353–367.

England, P.C. and Richardson, S.W., The Influence of Erosion upon the Mineral Facies of Rocks from Different Metamorphic Environments, *J. Geol. Soc.* (London), 1977, vol. 134, pp. 201–213.

England, P.C. and Thompson, A.B., Pressure–Temperature–Time Paths of Regional Metamorphism: I. Heat Transfer during the Evolution of Regions of Thickened Continental Crust, *J. Petrol.*, 1984, vol. 25, part 4, pp. 894–928.

Ferry, J.M. and Spear, F.S., Experimental Calibration of the Partitioning of Fe and Mg between Biotite and Garnet, *Contrib. Mineral. Petrol.*, 1978, vol. 66, pp. 113–117.

Fonarev, V.I., Graphchikov, A.A., and Konilov, A.N., A Consistent System of Geothermometers for Metamorphic Complexes, *Int. Geol. Rev.*, 1991, vol. 33, no. 8, pp. 743–783.

Ganguly, J. and Saxena, S.K., Mixing Properties of Aluminosilicate Garnets: Constraints from Natural and Experimental Data, and Applications to Geothermobarometry, *Am. Mineral.*, 1984, vol. 69, no. 1/2, pp. 88–97.

Golionko, G.B. and Krestin, E.M., Tectonics of the Crystalline Basement of the Northern Part of the Kursk–Voronezh Massif and Its Framing, *Izv. Vyssh. Uchebn. Zaved., Geol. Razved.*, 1975, no. 1, pp. 29–37.

Golionko, G.B., Efimkin, N.S., Zin'kovskii, V.E., and Krestin, E.M., Deep Geologic Structure of the Northeastern Slope of the Voronezh Massif and Pachelmskii Depression (Evidence from GSS), *Geotektonika*, 1973, no. 2, pp. 35–40.

Grafchikov, A.A. and Fonarev, V.I., Garnet–Orthopyroxene–Plagioclase–Quartz Geobarometer, in *Ocherki Fiziko-Khimicheskoi Petrologii* (Contributions to Physicochemical Petrology), 1991, no. 16, pp. 199–226.

Harley, S.L. and Green, D.H., Garnet–Orthopyroxene Barometry for Granulites and Peridotites, *Nature* (London), 1982, vol. 300, pp. 697–701.

Harley, S.L., The Origins of Granulites: a Metamorphic Perspective, *Geol. Mag.*, 1989, vol. 126, no. 3, pp. 215–247.

Harley, S.L., The Solubility of Alumina in Orthopyroxene Coexisting with Garnet in $FeO–MgO–Al_2O_3–SiO_2$ and $CaO–FeO–MgO–Al_2O_3–SiO_2$, *J. Petrol.*, 1984, vol. 25, no. 3, pp. 665–694.

Hodges, K.V. and Spear, F.S., Geothermometry, Geobarometry and the Al_2SiO_5 Triple Point at Mt. Moosilauke, New Hampshire, *Am. Mineral.*, 1982, vol. 67, no. 11/12, pp. 1118–1134.

Holdaway, M.J. and Lee, S.M., Fe–Mg Cordierite Stability in High-Grade Pelitic Rocks Based on Experimental, Theoretical, and Natural Observations, *Contrib. Mineral. Petrol.*, 1977, vol. 63, pp. 175–198.

Koziol, A.M. and Newton, R.C., Redetermination of the Anorthite Breakdown Reaction and Improvement of the Plagioclase–Garnet–Al_2SiO_5–Quartz Geobarometer, *Am. Mineral.*, 1988, vol. 73, pp. 216–223.

Lavrent'eva, I.V. and Perchuk, L.L., Phase Equilibria in the System Biotite–Garnet: Experimental Data, *Dokl. Akad. Nauk SSSR*, 1981, vol. 260, no. 3, pp. 731–734.

Nadezhka, L.I., Dubyanskii, A.I., Tarkov, A.P., *et al.*, Some Characteristics of the Deep Structure of the Voronezh Crystalline Massif, *Litosfera Tsentral'noi i Vostochnoi Evropy: Vostochno-Evropeiskaya platforma* (Lithosphere of Central and Eastern Europe: East European Platform), Sollogub, V.B., Ed., Kiev: Naukova dumka, 1989, pp. 121–135.

Nisbet, E.G., The Continental and Oceanic Lithosphere in Archean: Isostatic, Thermal and Tectonic Models, *Can. J. Earth Sci.*, 1984, vol. 21, pp. 1426–1441.

Novikova, A.S. and Shchipanskii, A.A., Tectonics of the Early Proterozoic Iron-Ore Basins: Kursk–Krivoi Rog and Khamersli–Naberu (Western Australia), *Geotektonika*, 1988, no. 3, pp. 49–61.

Nozhkin, A.D. and Krestin, E.M., *Radioaktivnye elementy v porodakh rannego dokembriya (na primere KMA)* (Radioactive Elements in Early Precambrian Rocks: An Example from KMA), Moscow: Nauka, 1984.

Perchuk, L.L., Derivation of Internally Consistent Fe–Mg Geothermometers on the Basis of Nernst's Law: A Revision, *Geokhimiya*, 1989, no. 5, pp. 611–622.

Perkins, D., III, and Ciphera, S.J. Garnet–Orthopyroxene–Plagioclase–Quartz Barometry: Refinement and Application to the English River Subprovince and the Minnesota River Valley, *Contrib. Mineral. Petrol.*, 1985, vol. 89, pp. 69–80.

Perkins, D., III, and Newton, R.C., Charnockite Geobarometers Based on Coexisting Garnet–Pyroxene–Plagioclase–Quartz, *Nature* (London), 1981, vol. 292, no. 9, pp. 144–146.

Pigage, L.C., and Greenwood, H.J., Internally Consistent Estimates of Pressure and Temperature: the Staurolite Problem, *Am. J. Sci.*, 1982, vol. 282, no. 7, pp. 943–969.

Sandiford, M. and Powell, R., Deep Crustal Metamorphism during Continental Extension: Modern and Ancient Examples, *Earth Planet. Sci. Lett.*, 1986, vol. 79, pp. 151–158.

Sandiford, M., Horizontal Structures in Granulite Terrains: A Record of Mountain Building or Mountain Collapse? *Geology*, 1989, vol. 17, pp. 449–452.

Savko, K.A. and Lebedev, I.P., Petrology of the Archean Phlogopite–Diopside Marbles of the Bryansk Block of the Voronezh Crystalline Massif, *Vestn. Voronezh. Univ., Ser. Geol.*, 1996, no. 2, pp. 32–41.

Sen, S.K. and Bhattacharya, A., An Orthopyroxene–Garnet Thermometer and Its Application for the Madras Charnockites, *Contrib. Mineral. Petrol.*, 1984, vol. 88, pp. 64–71.

Shchegolev, I.N., *Zhelezorudnye mestorozhdeniya dokembriya i metody ikh izucheniya* (Some Precambrian Deposits and Methods of Their Investigation), Moscow: Nedra, 1985.

Tarkov, A.P., *Glubinnoe stroenie Voronezhskogo massiva po geofizicheskim dannym* (Deep Structure of the Voronezh Massif: Geophysical Evidence), Moscow: Nedra, 1974.

Thompson, P.H., Moderate Overthickening of Sialic Crust and the Origin of Granitic Magmatism and Regional Metamorphism in Low-P–High-T Terranes, *Geology*, 1989, vol. 17, pp. 520–523.

Wells, P.R.A., Thermal Models for the Magmatic Accretion and Subsequent Metamorphism of Continental Crust, *Earth Planet. Sci. Lett.*, 1980, vol. 46, pp. 253–265.